Electron Linacs for Research and Applications

Steve Lidia

This material is based upon work supported by the U.S. Department of Energy Office of Science under Cooperative Agreement DE-SC0000661, the State of Michigan and Michigan State University. Michigan State University designs and establishes FRIB as a DOE Office of Science National User Facility in support of the mission of the Office of Nuclear Physics.

Outline

- Facts about electrons
- Types of electron linacs and examples
  - Room Temperature Linacs
  - Superconducting Linacs
  - Recirculating and Energy Recovery Linacs
  - Induction Linacs
  - Plasma accelerators
- Applications
  - HEP, NP
  - Radiation production
  - Industrial
  - Medical
  - Homeland security, Stockpile stewardship
- Injectors and beam sources
  - Thermionic, field emission, photoemission
- Collective effects in linacs
  - Space charge
  - Emittance compensation
  - Emittance exchange
  - BBU and suppression techniques
  - Energy spread growth

Electrons Are Light
Velocity is Nearly Equal to Speed of Light

- Electrons are light mass particles. They move with the speed of nearly equal to the speed of light after going through several cavities

$\beta = \sqrt{1 - \left(\frac{mc^2}{E}\right)^2}$, for energy 10 MeV, $\beta \approx 0.999$

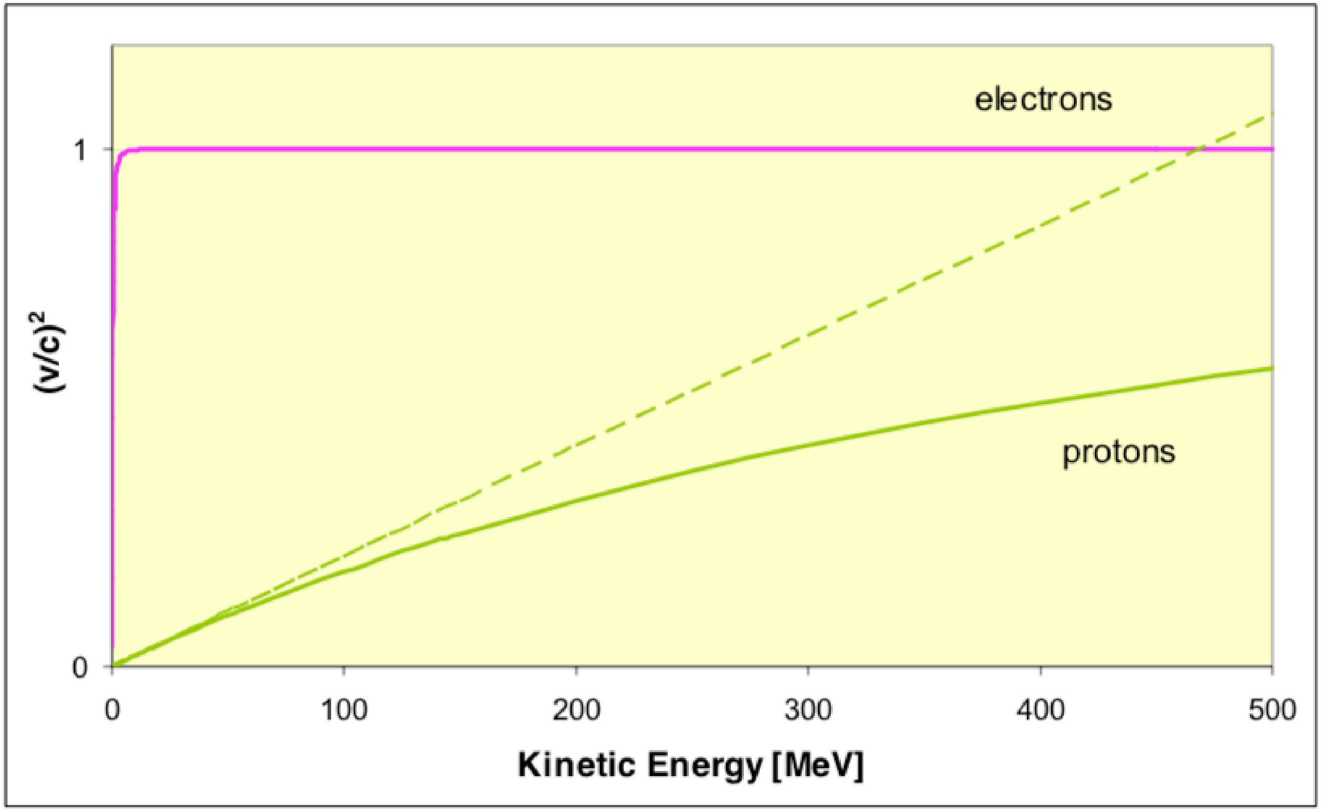

Phase/Energy Motion is "Frozen" in E-Linacs

$$\frac{d\Delta E}{ds} = e\mathcal{E}\left(\sin(\phi_s + \Delta\phi) - \sin\phi_s\right)$$

$$\frac{d\Delta\phi}{ds} = -\frac{\omega}{mc^3\beta_s^3\gamma_s^3}\Delta E$$

Y. Hao

$$\frac{d^2\Delta E}{ds^2} = -\frac{e\mathcal{E}\omega\cos\phi_s}{mc^3\beta_s^3\gamma_s^3}\Delta E$$

$$k_s^2 = \frac{e\mathcal{E}\omega\cos\phi_s}{mc^3\beta_s^3\gamma_s^3} \qquad k_s \to 0 \; as \; \gamma \to \infty$$

- Synchrotron (Phase/Energy) motion in e-linacs slows down as the energy increases. This allows acceleration on-crest (maximum energy gain, no longitudinal focusing).
- Phase motion and longitudinal phase space manipulation is still possible in dispersive areas (bends) where path length depends on particle energy. Such manipulations require correlated energy spread and off-crest acceleration or dedicated cavities. Example: bunch compression chicanes

Electron beam intensity: tenuous to dense

- Measure of collective effects
  - Self-fields and beam distribution affect the local balance of forces
  - Modulated beams with high peak currents drive localized impedances
    - » Power transfer and feedback between beam and environment
- Generalized 'perveance' from microwave electronics theory
  - Measure of strength of self-fields $K = \frac{I}{I_0}\frac{2}{\beta^3\gamma^3}(1-\gamma^2 f_e)$
    - » $I_0 = \frac{4\pi\varepsilon_0 mc^3}{q} \approx 17.03\ kA\ (electrons)$
    - » f_e is the degree of neutralization present in the channel $(0 < f_e < 1)$
- Envelope vs. Betatron description of transverse motion
  - $\sigma_r'' + \left(\frac{\gamma'}{\gamma\beta^2}\right)\sigma_r' + \left[k_\beta^2 + \frac{\gamma''}{2\gamma\beta^2}\right]\sigma_r - \frac{K}{\sigma_r} - \left[\frac{\varepsilon_{nr}^2}{\beta^2\gamma^2} + \frac{\langle p_\theta\rangle^2/m^2c^2}{\beta^2\gamma^2}\right]\frac{1}{\sigma_r^3} = 0$
  - $2\beta_x\beta_x'' - (\beta_x')^2 + 4k_\beta^2\beta_x^2 = 4\ ,\ \varphi_x' = {}^1/_{\beta_x}$ (no x/y coupling, no space charge)

Beam Transport

- Envelope description

$$\sigma_r'' + \left(\frac{\gamma'}{\gamma\beta^2}\right)\sigma_r' + \left[k_\beta^2 + \frac{\gamma''}{2\gamma\beta^2}\right]\sigma_r - \frac{K}{\sigma_r} - \left[\frac{\varepsilon_{nr}^2}{\beta^2\gamma^2} + \frac{\langle p_\theta\rangle^2/m^2c^2}{\beta^2\gamma^2}\right]\frac{1}{\sigma_r^2} = 0$$

- Identify the terms

- Steady-state or matched envelope solution for constant focusing channel

  - $\sigma_r'' = 0;\ \sigma_r' = 0$ ⇨ $\left[k_\beta^2 + \frac{\gamma''}{2\gamma\beta^2}\right]\sigma_r - \frac{K}{\sigma_r} - \left[\frac{\varepsilon_{nr}^2}{\beta^2\gamma^2} + \frac{\langle p_\theta\rangle^2/m^2c^2}{\beta^2\gamma^2}\right]\frac{1}{\sigma_r^2} = 0$

  - Coasting solution ($\gamma'' = 0$) $k_\beta^2\sigma_r^3 - K\sigma_r - \frac{\varepsilon_{n,eff}^2}{\beta^2\gamma^2} = 0$ Emittance v. Space-charge dominated transport

Types of Electron Linacs and Examples

Traveling and Standing Wave Structures (Refresher)

V. Yakovlev

RF linear accelerators

- Travelling wave accelerators.

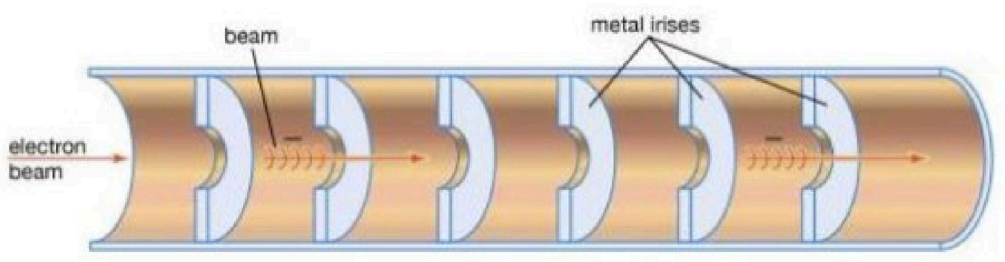

The wave propagates left to right.

- Standing wave accelerators.

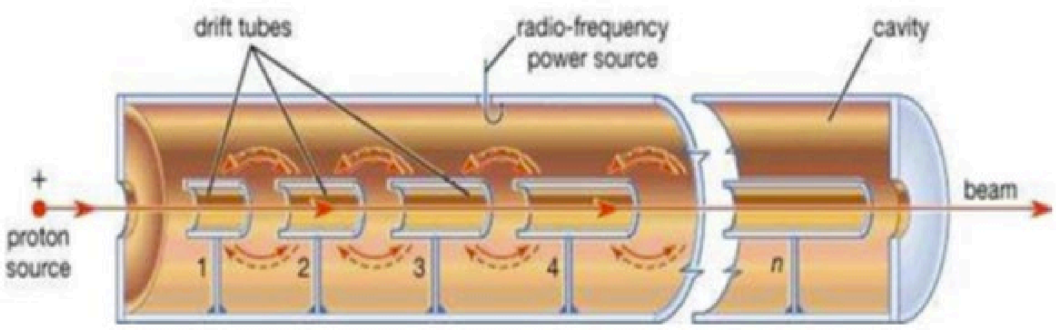

Maximum gradients ~100 MV/m

RF Pulses propagating along RF structure. Beam velocity equals to RF phase velocity. Structures are transparent for RF pulses at specific frequencies only.

A standing wave is a superposition of two traveling waves going in opposite directions. A standing wave fills in the whole structure, resonating at one of the modes. Modes and geometry are selected to be synchronous with the beam.

Types of Accelerating Cavities and Structures
RT Traveling Wave Cavity (Refresher)

V. Yakovlev

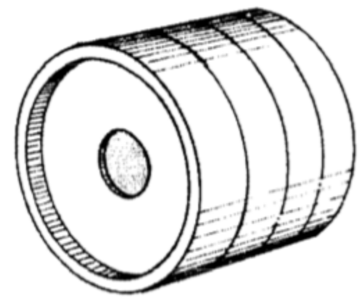

I. DISK-LOADED STRUCTURE

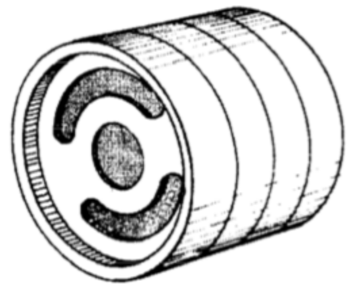

6. SLOTTED DISK STRUCTURE

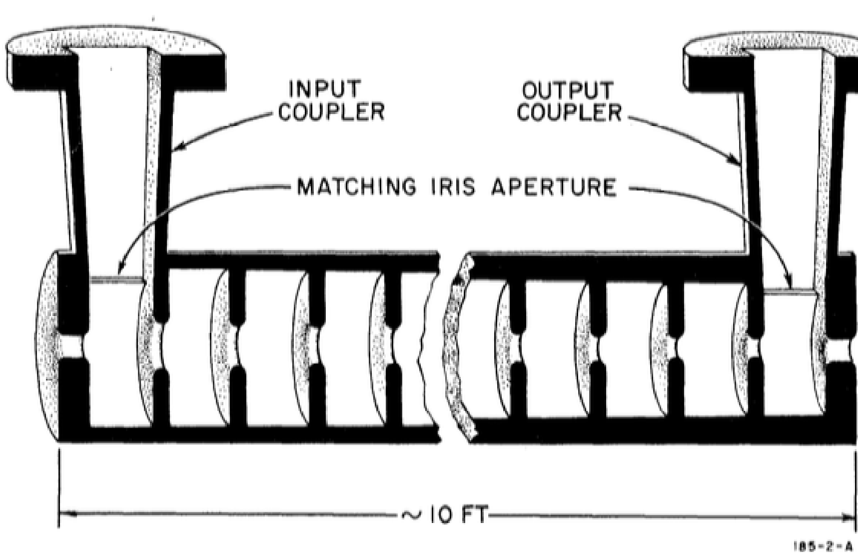

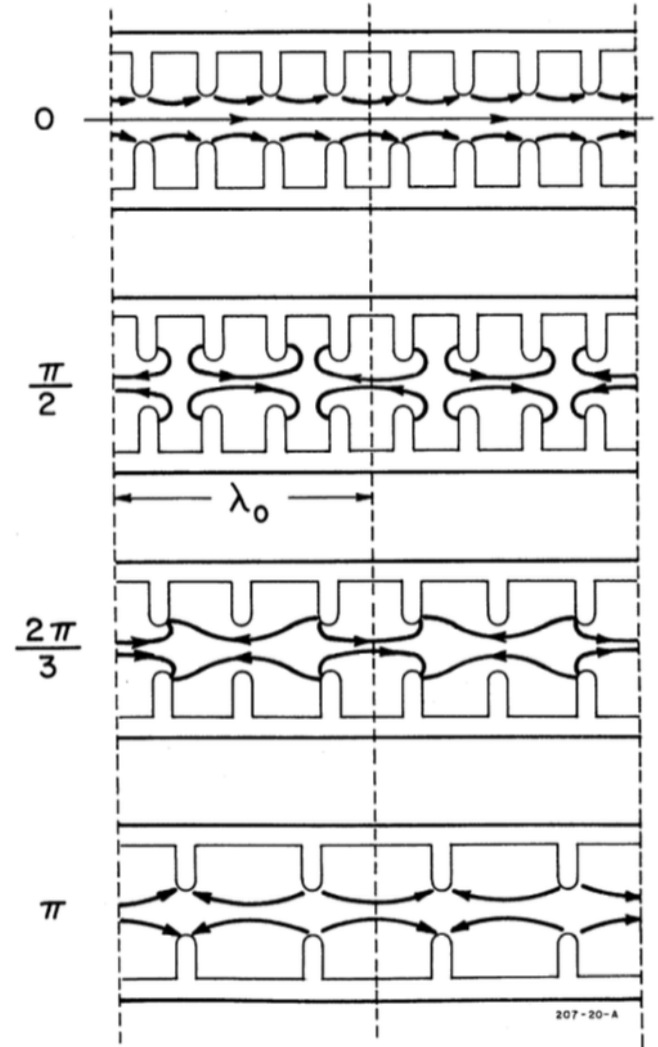

Types of Accelerating Cavities and Structures SRF Cavity (Refresher)

V. Yakovlev

Superconducting ILC 9 cell cavity Operating in π-mode, standing wave mode.

SC cavities are operated in standing wave mode

Input RF power

Slowed down by factor of approximately $4x10^9$

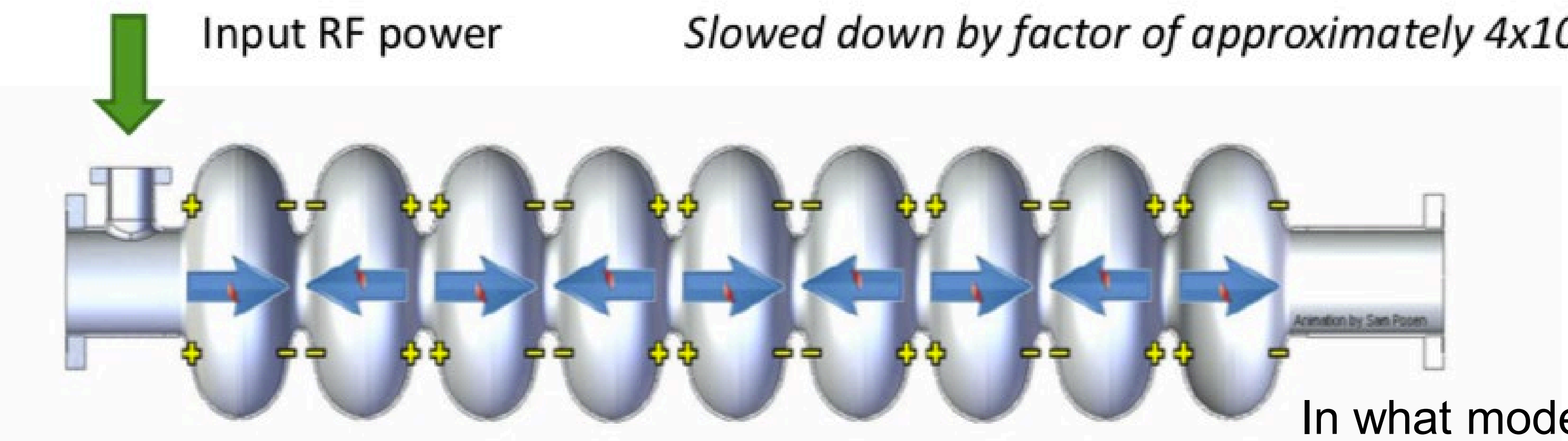

In what mode is this cavity oscillating?

Induction Linacs
Long Pulse kA beams

- Used for accelerating pulsed, high beam currents (10's kA) to multi-MeV
  - Beam power in GW over 100s ns
- Acceleration gradients ~250 kV/gap
- Pulsed x-radiography and nuclear effects studies

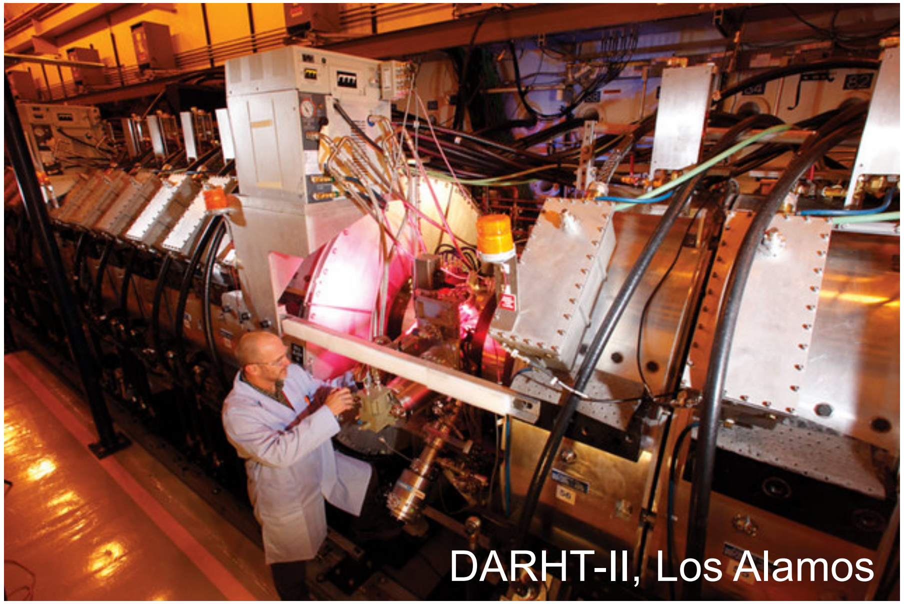

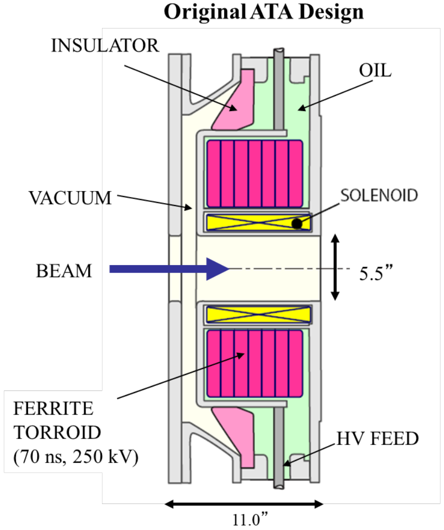

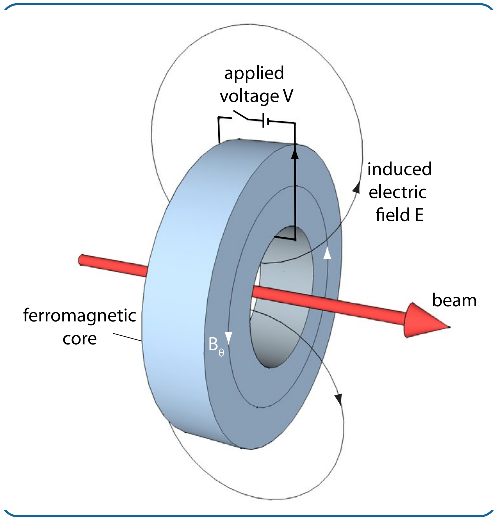

$$\nabla \times \vec{E} = -\frac{\partial}{\partial t}\vec{B} \Rightarrow \oint_C \vec{E} \cdot d\vec{l} = -\frac{\partial}{\partial t}\int_A \vec{B} \cdot d\vec{A}$$

$$\int V\,dt = \text{'volt-seconds'} = \int_A \vec{B} \cdot d\vec{A} = \Delta B_\theta A_{core}$$

ΔB_θ is the core flux swing < $2B_{sat}$

B_{sat} is the material saturation field ($\mu \sim \mu_0$) and is ~0.4 T for ferrite up to ~2 T for glassy metals (eg. 2605SC MetGlas).
Cores must be 'reset' between pulses.

Plasma Accelerators

1 TeV/m

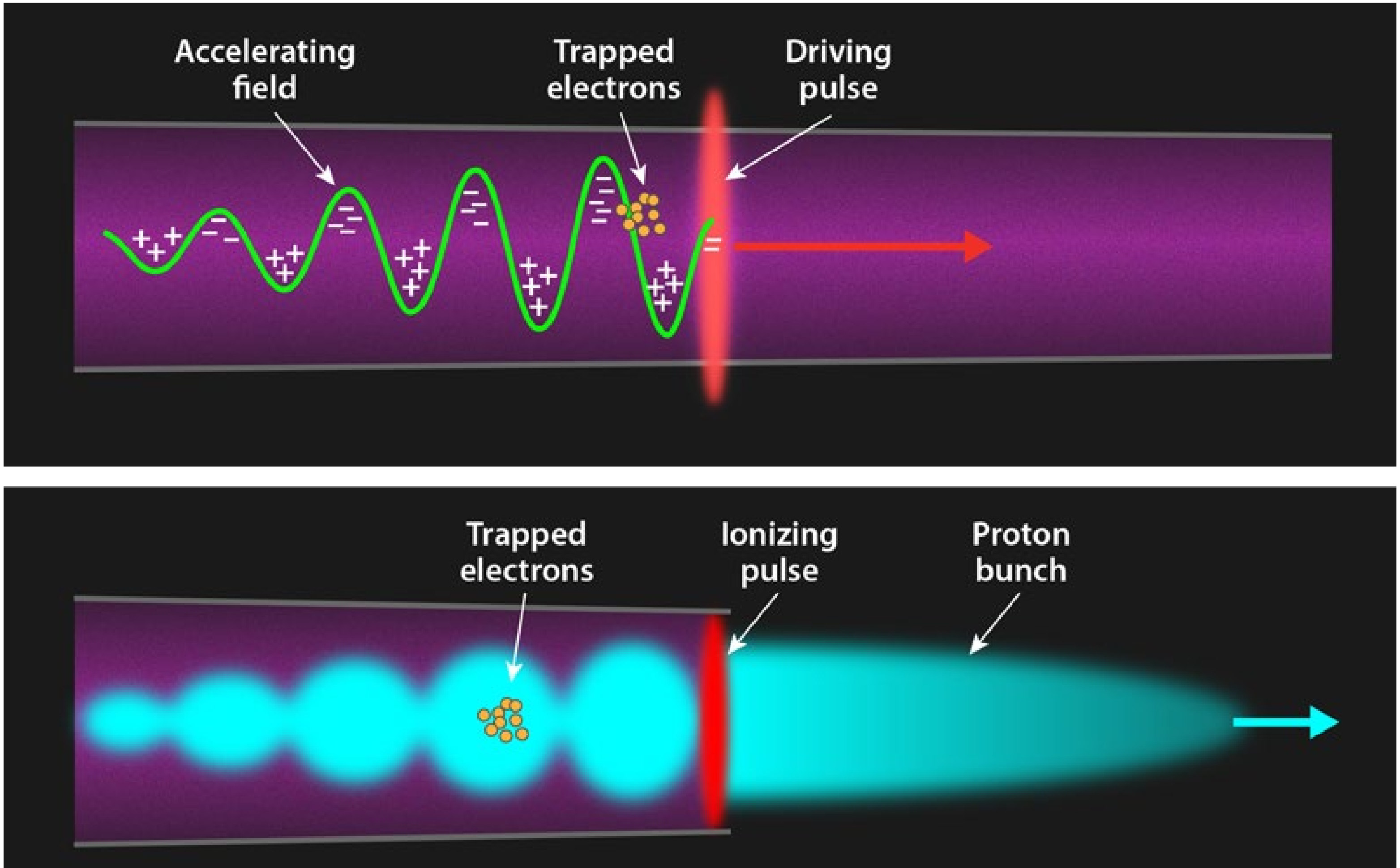

https://physics.aps.org/articles/v12/19#

8 GeV with 850 TW laser acceleration

https://doi.org/10.1103/PhysRevLett.122.084801

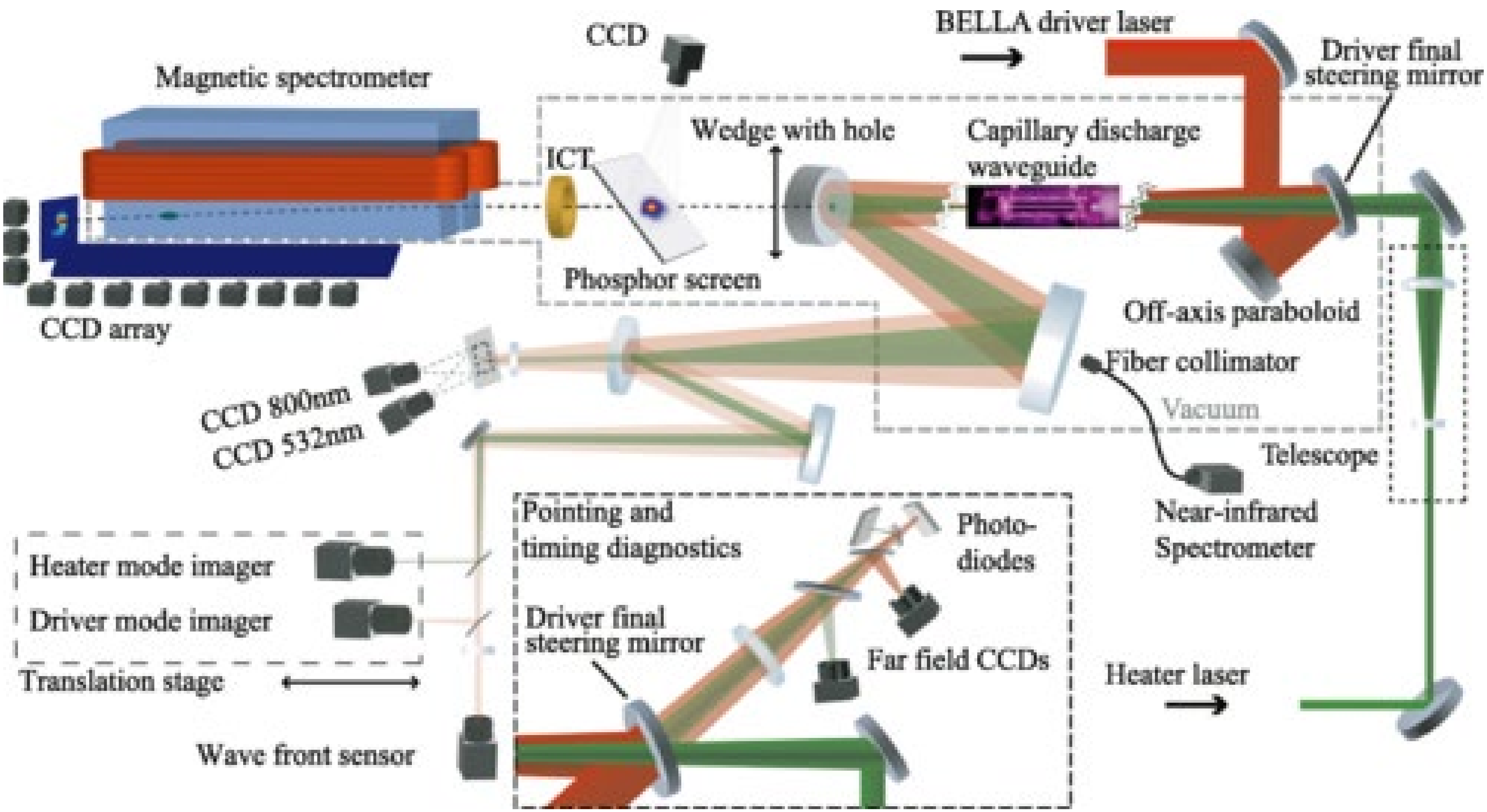

Laser-Plasma Electron beam quality

https://doi.org/10.1103/PhysRevLett.122.084801

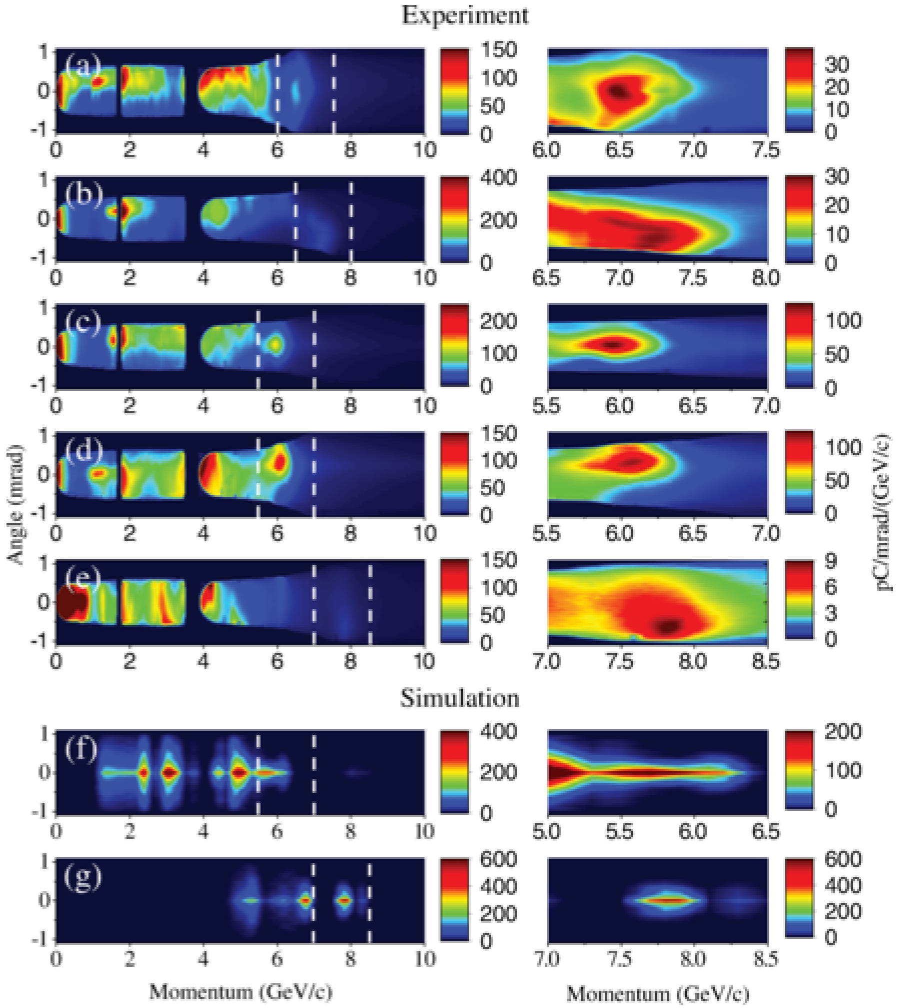

(a)–(e): Electron beams measured by the magnetic spectrometer for n0=3.4 × 1017 cm−3 , rm=69 μm and laser power 850 TW.

The driver laser pulse arrival was timed with the peak of the heater pulse. The heater pulse arrived 300 ns after the peak of the discharge current, except for (e), where the delay was 420 ns, and the heater-induced density reduction was measured to be larger, with n0=2.7 × 1017 cm−3 and rm=61 μm .

The white dashed lines show the regions that are plotted in the right hand column, which shows the detailed spectrum of the highest energy peaks.

The electron beam spectrum simulated by INF&RNO using the MARPLE-retrieved density profile (with n0=3.4 × 1017 cm−3) is shown in (f).

In (g) a simulation is shown for the parameters of (e) using a transversely parabolic and longitudinally uniform density profile.

Accelerator on a Chip
Dielectric Wall Accelerators

SLAC

Modelocked Thulium Fiber Laser (λ = 2μm, 10μJ, $300k)

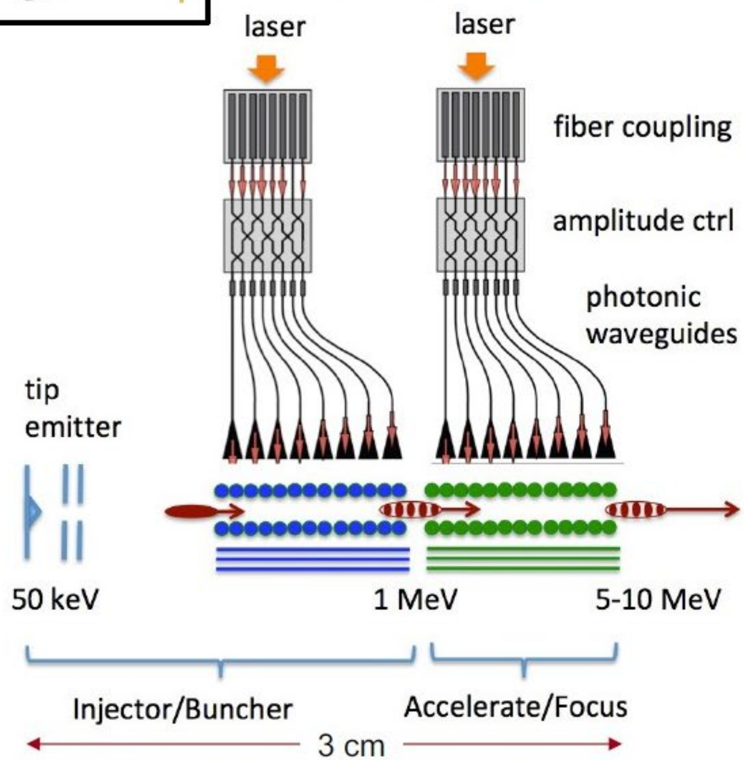

Required lasers are MHz rep rate, low pulse energy, wallplug efficiency ~ 30%

Dielectric materials can withstand GV/m fields and kilowatts of average power

Can be mass produced using techniques of the integrated circuit industy.

SEM images of DLA prototypes tested at SLAC

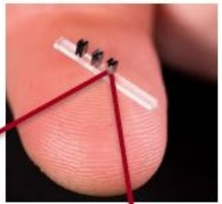

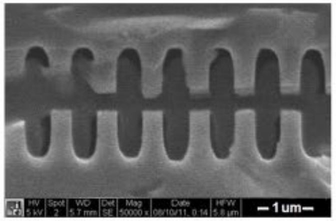

fused silica

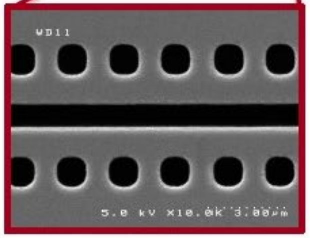

silicon

DLA research aims to produce ultracompact nanofabricated devices for particle acceleration, powered by efficient solid-state lasers.

Applications of Electron Linacs

Range of Electron Linac Applications

	Low Intensity (uA-A)	High Intensity (A-kA)	Very High Intensity (kA-MA)
Low Energy (< MeV)	Semiconductor processing and metrology; Streak cameras; Ultrafast electron diffraction	Microwave production, Welding, Irradiation, Medical treatment	
High Energy (< GeV)	Electron cooling, Nuclear physics, Medical isotope production	Two-beam accelerators	Flash X-radiography, Fusion effects
Very High Energy (> GeV)	Linear colliders	X-ray FEL drivers	

Industrial Linacs
Example: Medical Linacs

- Medical electron accelerators are used for cancer treatment
  - Electron beam is used to produce bremsstrahlung photons
- Medical accelerators are relatively simple RT, disk-loaded copper structures with different coupling mechanisms between cells
- Typical energy of mass produced treatment systems is 5 – 10 MeV
- >5000 medical systems operated in the world in 2015

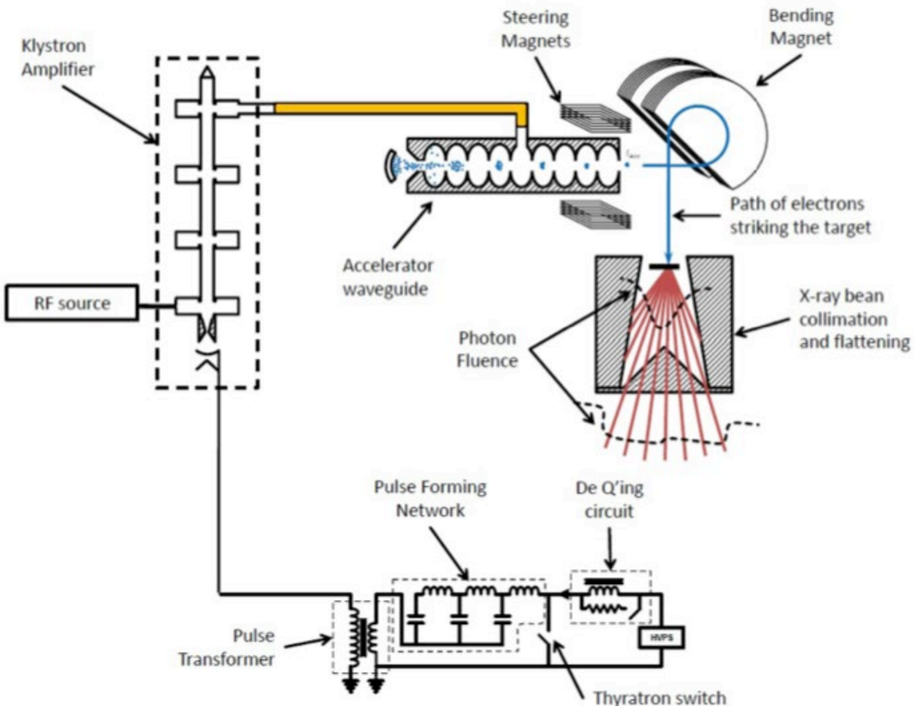

Superconducting Electron Linacs Example: EU-XFEL

EU-XFEL cryomodules in
The tunnel

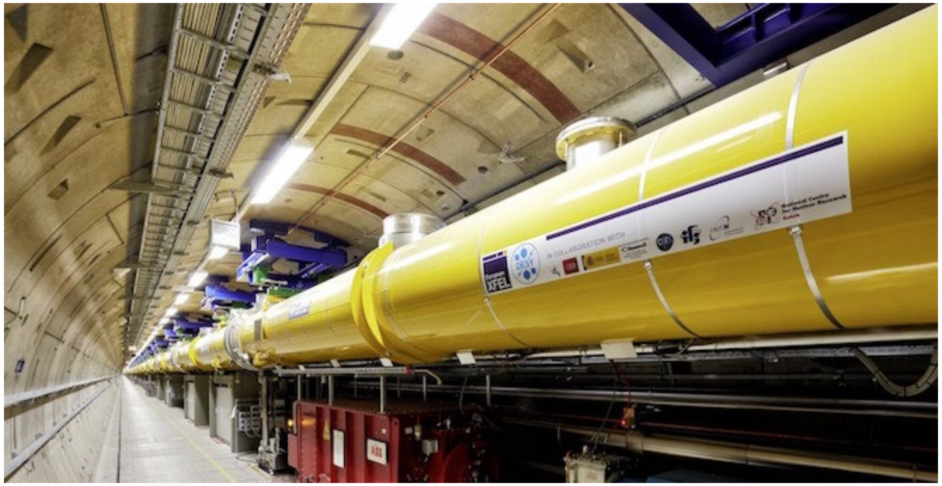

Location – near Hamburg, Germany

Start of construction - 2009
Commissioning completed - 2017

Energy – 17 GeV
Accelerator length – 1.7 km
Facility length – 3.4 km
Number of CMs – 96 + 2 (injector)
Cavities – TESLA type, 1.3 GHz, 8 per CM
Operational temperature – 2K
Operation mode – pulsed, bunch trains

EU-XFEL site
near Hamburg, Germany

EU-XFEL Linac Consists of 96 Joined CMs
Forming 1.7 km Long Uninterrupted Cold Linac

Number of CMs – 96 + 2 (injector)
Cavities – TESLA type, 1.3 GHz, 8 per CM
Operational temperature – 2K

EU-XFEL Cryomodule and Lattice

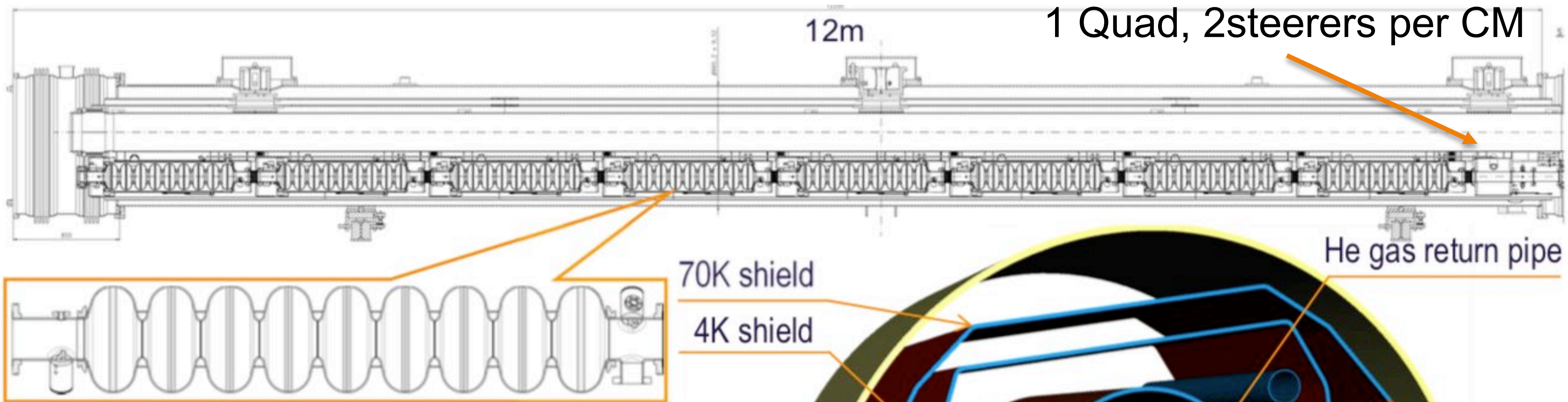

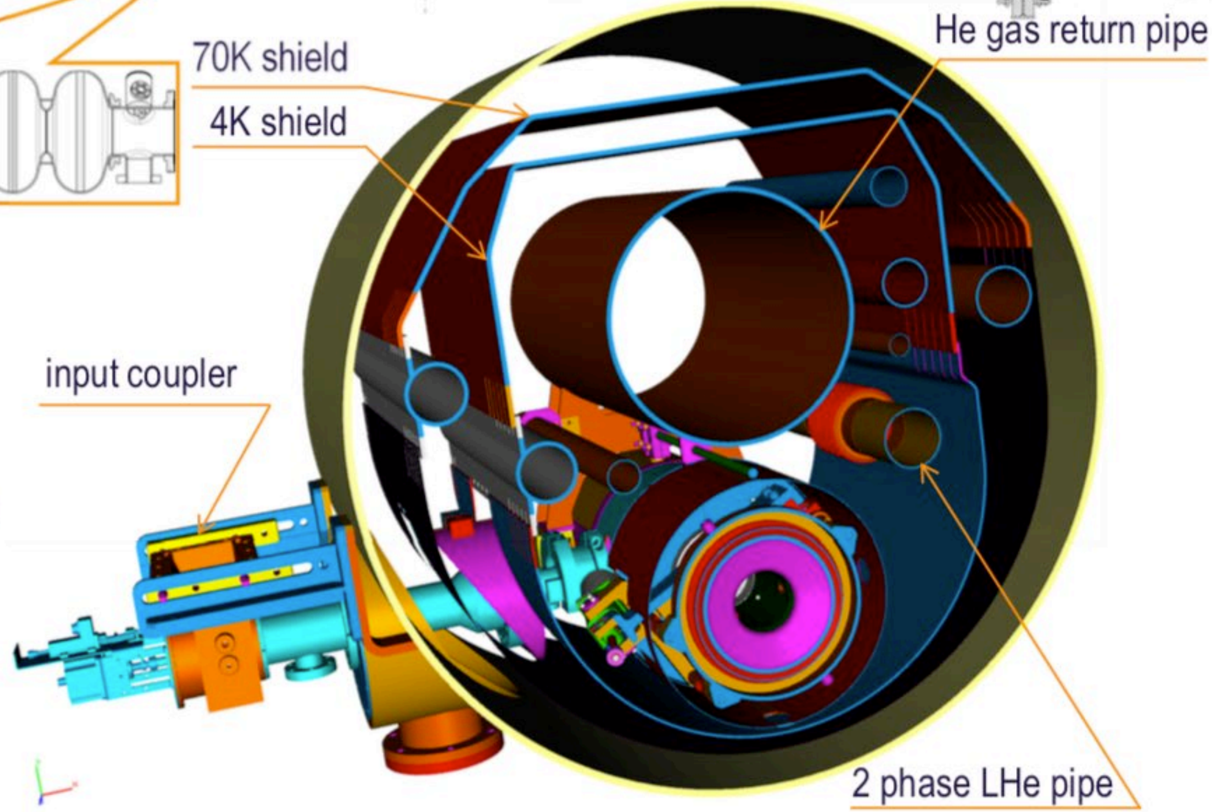

Cavity type	TESLA
Number of cavities	8
Cavity length	1.035 m
Operating frequency	1.3 GHz
R/Q	1030 Ω
Accelerating Gradient	20..31 MV/m
Quality factor	10^{10}
Q_{ext} (input coupler)	4.6×10^6
Operating temperature	2 K

LHe cooling 2K / 31mbar
HERA cryoplant is used

Warm Copper Linacs
Example: SLAC Two Mile Linac

Time Line
Proposal – 1957
Start of construction – 1962
Completion – 1966, >50 years
Upgrades – 1970s, 1980s, now

Principle parameters
Particles – e-, e+
Length – 3 km
Energy – ~50 GeV (1980s)
Acc. Grad. – 15 MeV/u
Peak power – 64 MW
Structure – Cu, disk-loaded
Pulse length – <2 us, 60 Hz
Pulse current – >50 mA

Program
Initial – Collider, Fixed target
Later – Up to 15 GeV Injector for multiple accelerators and driver for light sources

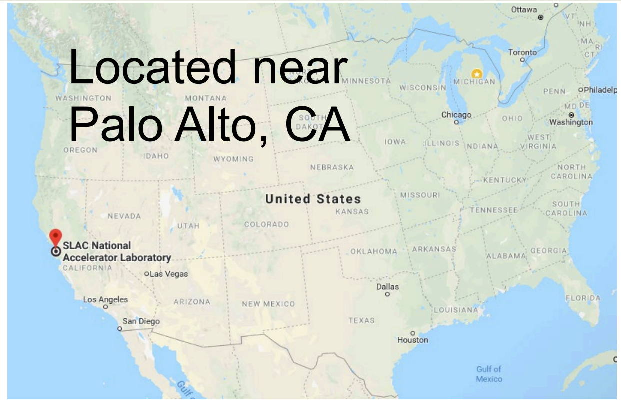

William Hansen, et al
Stanford University 1947
Mark I linac - 3.6m section produced 6 MeV electrons
Mark II 1949 klystron powered
Mark III 1950 10m 75 MeV
Mark IV 1954 20ft 80 MeV, SLAC prototype

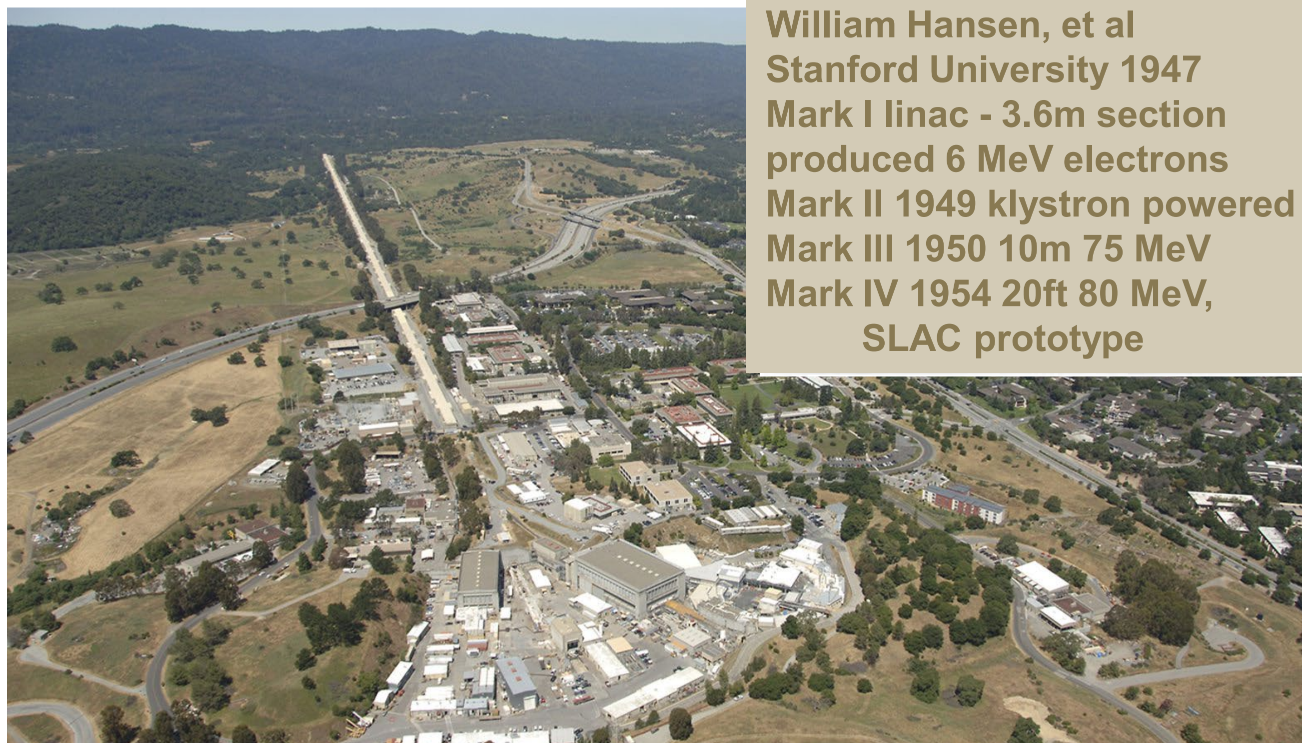

SLAC Accelerating Structure

Wavelength – ~10 cm
Frequency – 2856 MHz
Acc. Grad. – 15 MeV/m

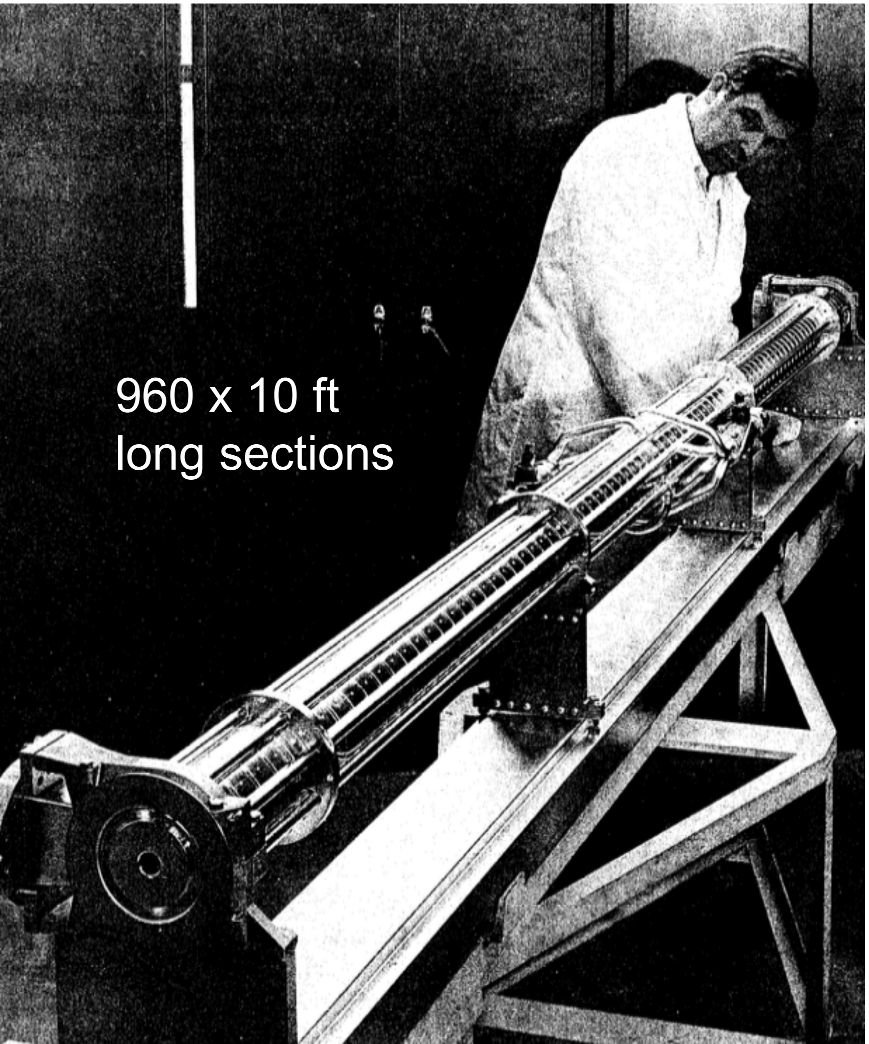

960 x 10 ft
long sections

Disk-loaded brazed copper structure

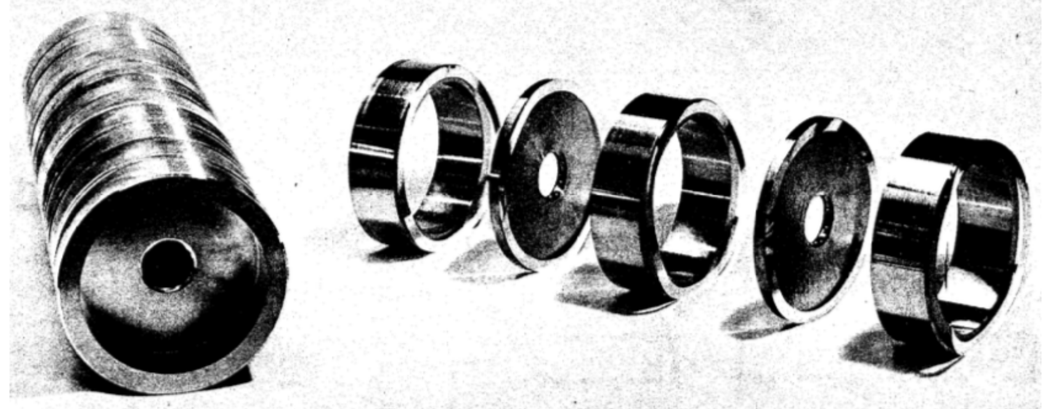

Diagnostics section
and Quad doublets
every 333 ft

SLAC Linac is Very Versatile Machine
Source of Positrons Gives Unique Opportunities

High Energy Physics Program, until 2008

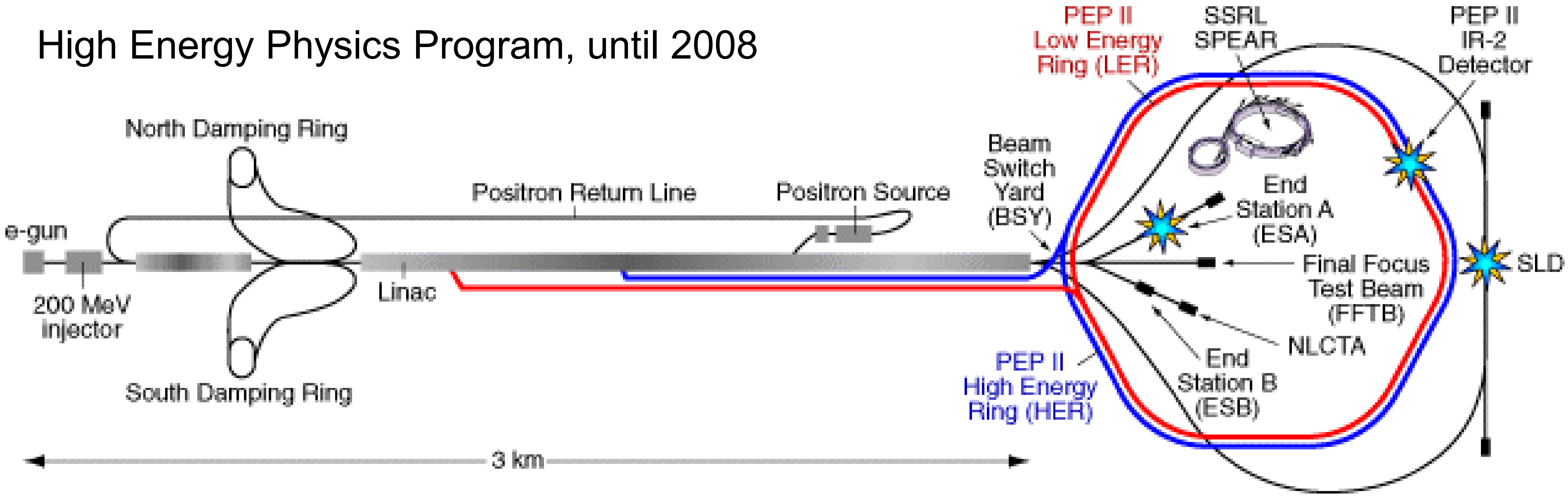

- Fixed target experiments with Electrons
- e+/e- collider linear (Z-W bosons) - First ‘linear’ collider
- SPEAR/SSRL (J/ψ charm quark – Nobel Prize 1976, tau-lepton – Nobel prize 1995), converted to light source with a dedicated injector. Contributed to Nobel Prize in Chemistry, 2006.
- PEP-II B-factory – precision heavy quark physics

e^+e^- Strawman Collider Geometry

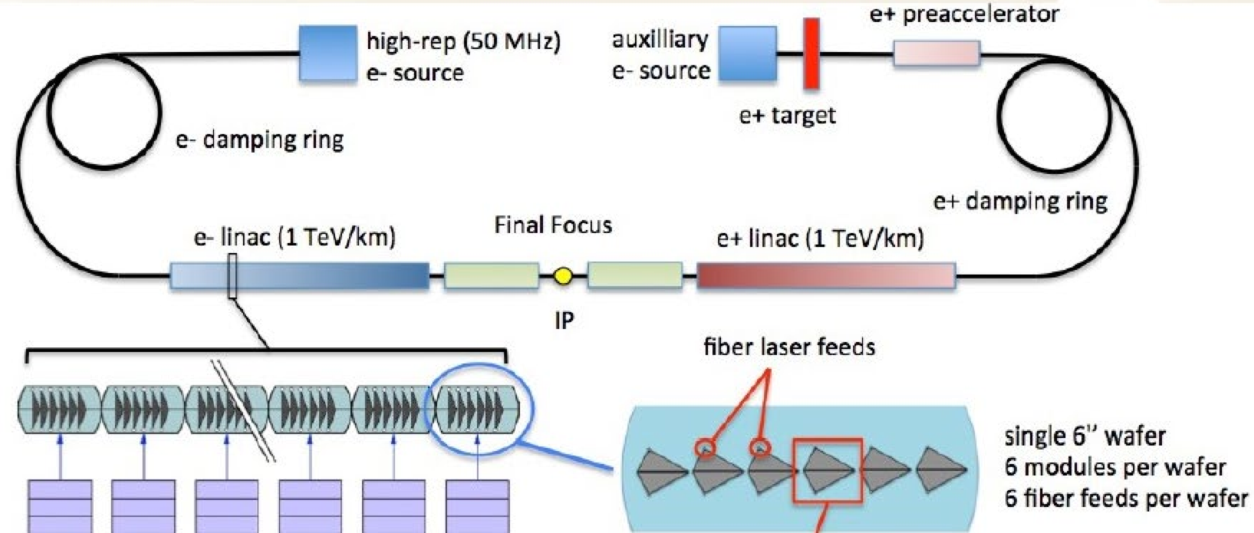

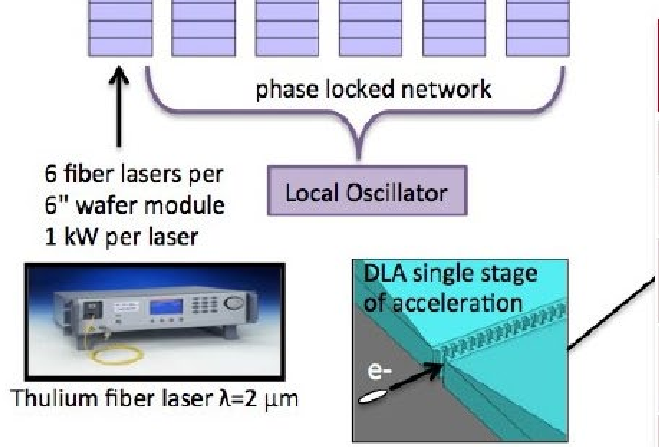

Parameter	Units	CLIC 3 TeV	DLA 3TeV	DLA 250 GeV
Bunch Charge	e	3.7e9	3.0e5	3.8e5
Rep Rate	MHz	5e-5	20	60
Beamstrahlung E-loss	%	**28.1**	**1.0**	**0.6**
Enhanced Luminosity / top 1%	cm-2/s	2.0e34	3.2e34	1.3e34
Wallplug Power	MW	582	374	152

LCLS and LCLS - II
From HEP to Light Source, From RT Linac to SC CW Linac

- Basic Energy Science (light source), currently leading program
- LCLS (Linac Coherent Light Source)
  - Photon energy – 200eV – 10keV
  - Pulse duration – femtosecond time scale – allows fast snapshots of dynamics systems.
- LCLS-II Upgrade will use SC linac and SC gun (from MSU!)

LCLS (Linac Coherent Light Source) and LCLS-II

Recirculating and Energy Recovery Linacs

The phase of the recirculated beam is determined by the length of the recirculating path.

The recirculated beam can be accelerated or decelerated depending on the phase (0° or 180°, respectively)

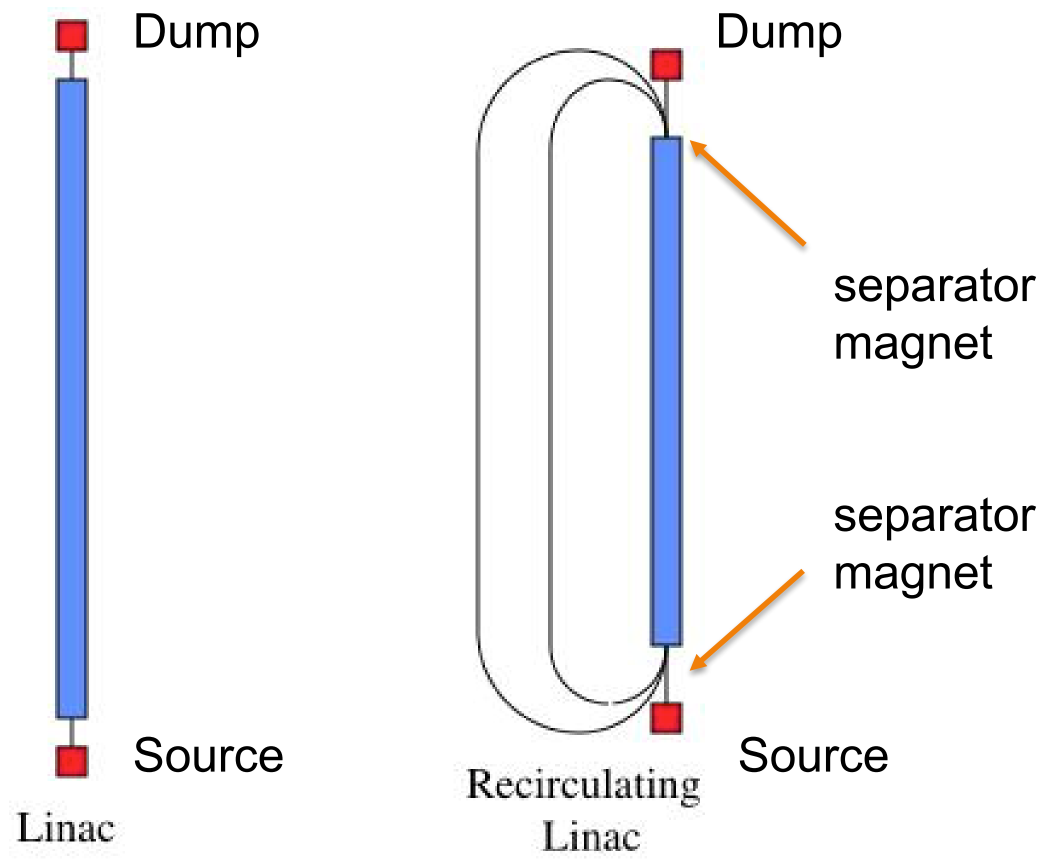

Magnet bending radius depends on beam energy. Bunches with different energy will travel on different paths. DC magnets are used.

Recirculating Linac
Example: CEBAF, Jefferson Lab

5 pass machine
Particles – electrons
E_{max} – 12 GeV
Operation mode - CW
Beam Power – 800 kW
Circumference – 0.9 mile

Two superconducting linacs
50 cryomodules:
40 Old type, 5-cell, 5-12 MeV/m
10 New type, 7-cell, 20 MeV/m
Frequency – 1497 MHz

Year Operational – 1995
Users/year – 1500 (2016)
4 halls in can be serviced simultaneously
Fixed target experiments and bremsstrahlung photons

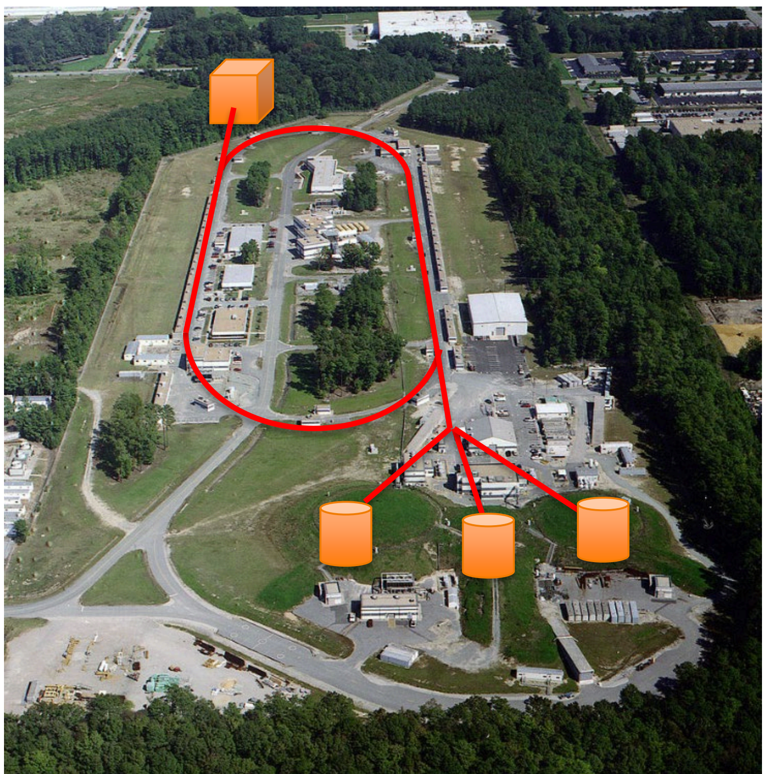

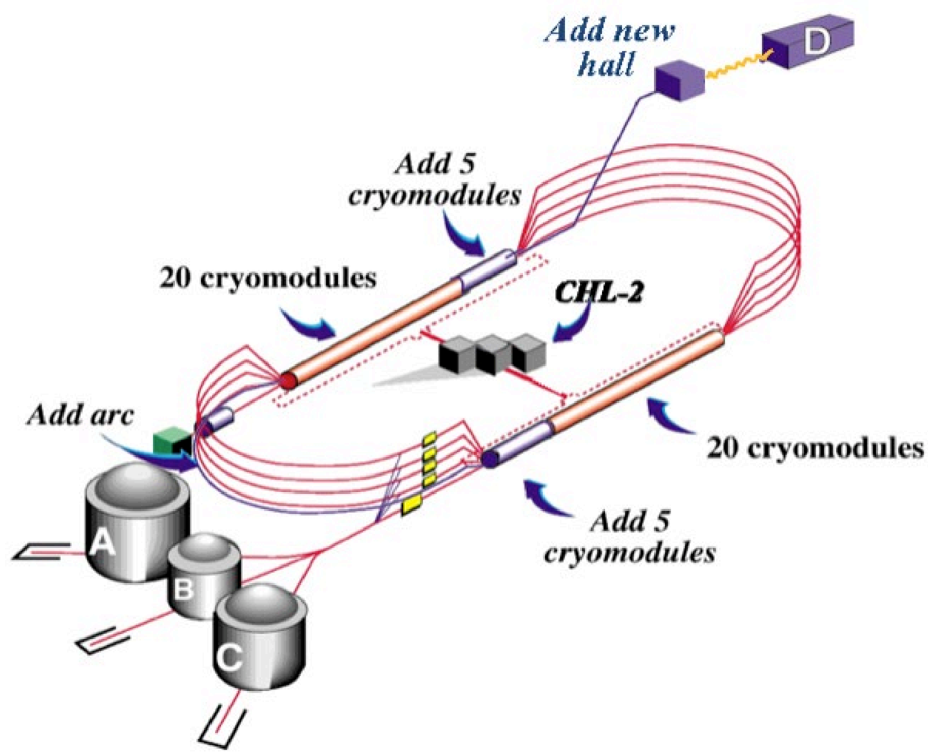

Sources of Electron Beam and Injectors

Types of Electron Guns

- Electron sources, frequently called guns, and injector systems are important sub-systems of electron linacs
  - Linacs can preserve beam quality during acceleration, making them attractive for various applications.
- Without a good source a linac cannot deliver high quality beam
- Main mechanisms to produce electron beam:
  - Thermionic (heated cathode like in a old CRT TV) – used for application that do not require good beam quality, e.g. bremsstrahlung photon production
  - Photoemission – can produce high quality beam, flexible time structure, require powerful laser
  - To increase beam ‘brightness’ current R&D focuses on laser-plasma and field emission sources
- Two main types of of electron guns
  - DC – using DC potential to accelerate electrons
  - RF – using RF cavity to accelerate electrons directly after cathode – increased accelerating gradient alleviates space charge (FEL)
    - » Room Temperature and Superconducting RF structures

Thermionic Electron Guns
Electrons are Emitted by a Hot Cathode

Principle diagram of
a thermionic DC gun

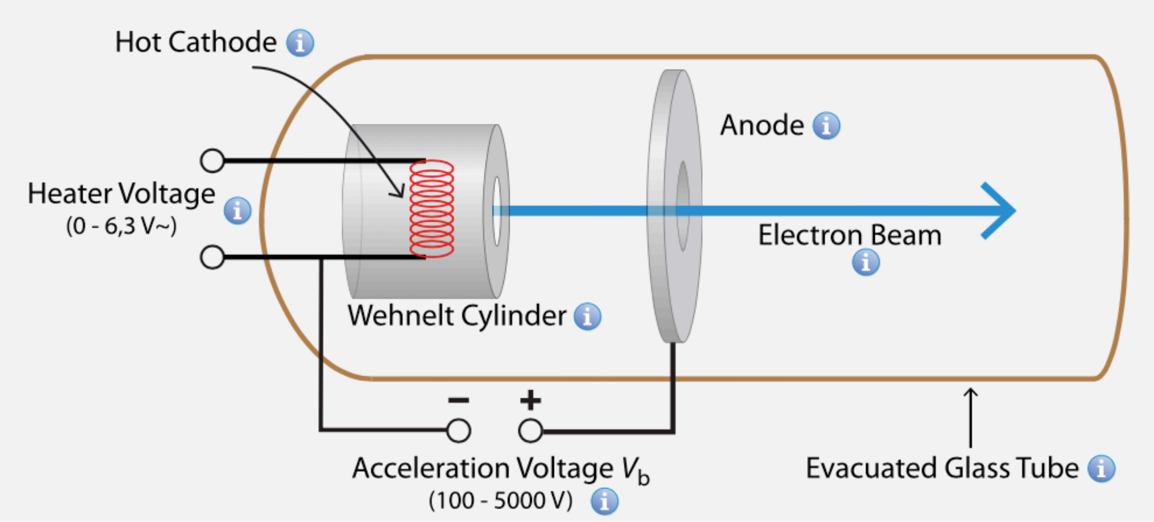

$$J = \frac{4\pi e m}{h^3}(k_B T)^2 exp\left[-\frac{\Phi}{k_B T}\right]$$
$$= A T^2 exp\left[-\frac{\Phi}{k_B T}\right]$$

Richardson-Dushman

Layout of a thermionic electron gun. RF electric field accelerates emitted electrons
Cavity material is copper.
1.5-cell cavity.

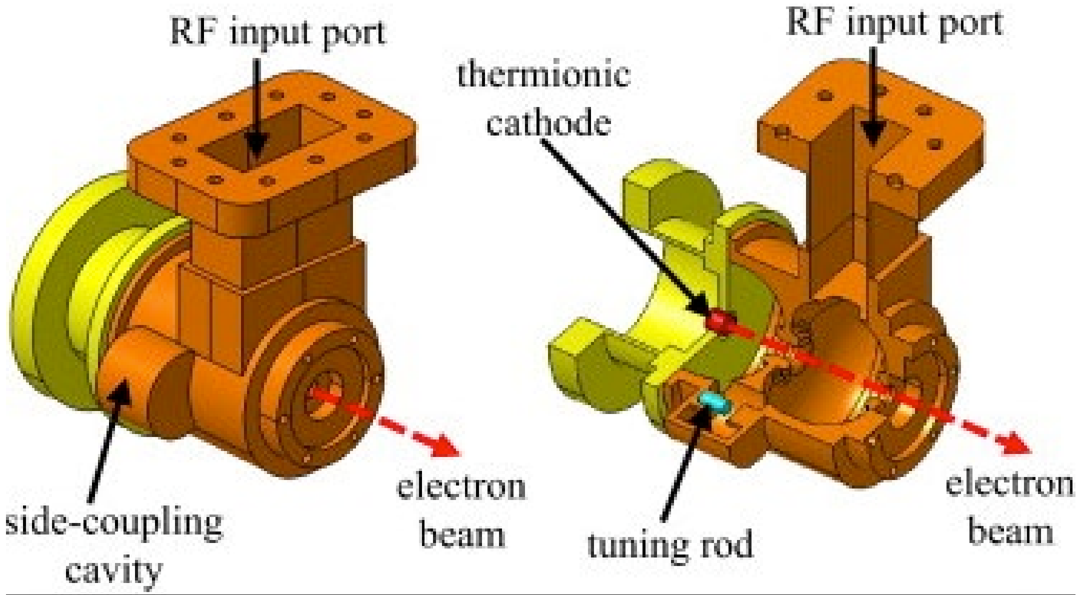

Photo-Emission Electron Guns

- Metal photocathodes
  - Material example: Pb, Cu, Ca, Mg, Ba, Nb
  - Require UV photons (>4.5 eV)
  - $<10^{-4}$ quantum efficiency (QE)
  - Short penetration depth (~14 nm)
  - Prompt electron emission
  - Larger transverse energy on emission

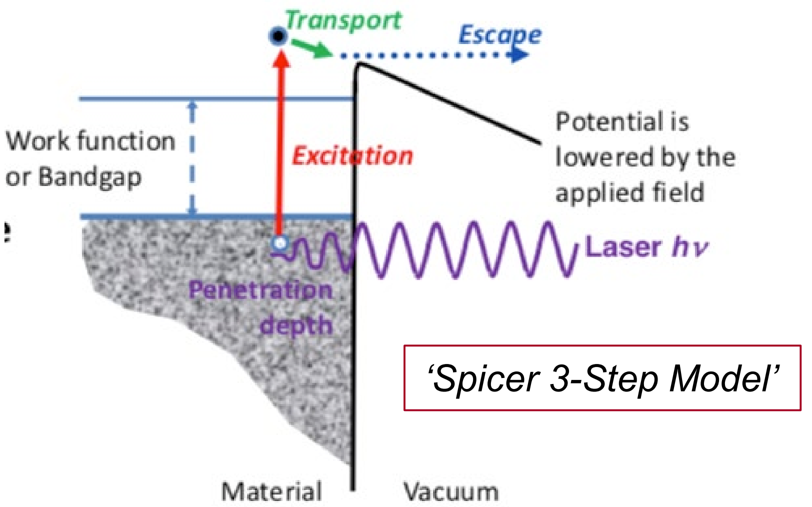

- Semiconductor photocathodes
  - Material:
    - » GaAs (Cs)
    - » Alkali-based: K_3Sb, Cs_2Te, other stoichiometric combinations
  - Require visible or UV photons
  - 1% - 50% quantum efficiency
    - » Highly dependent on vacuum
  - Can generate polarized electrons (strained lattices)
  - Long penetration depth (~mm)
  - Can have delayed electron emission (GaAs)
  - Can tailor bandgap to laser photon energies

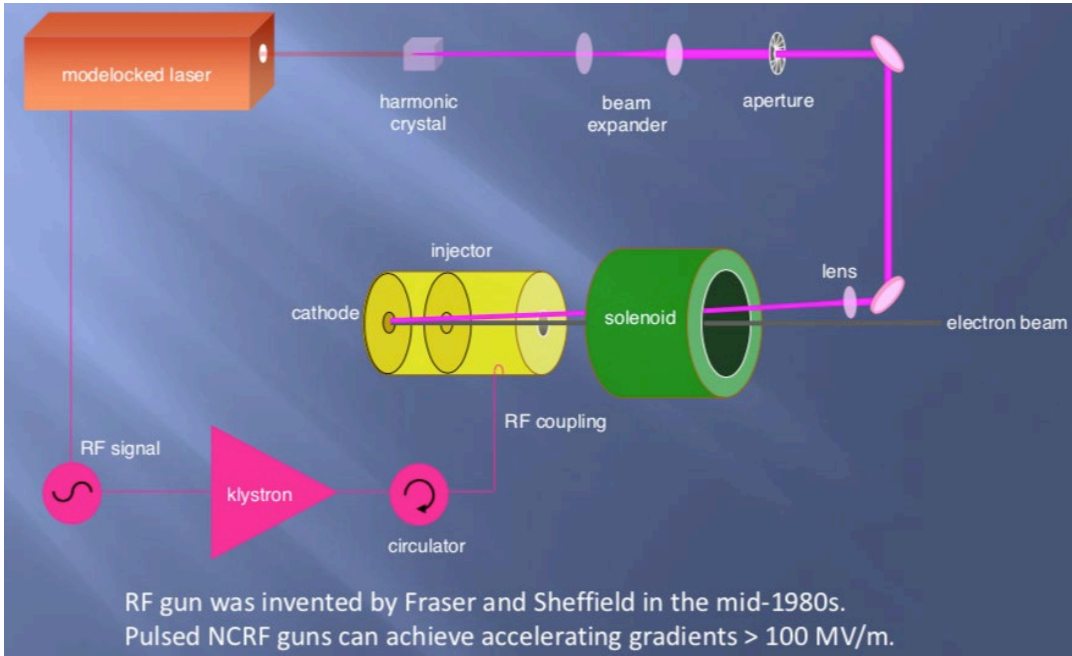

JLab FEL DC Photoinjector

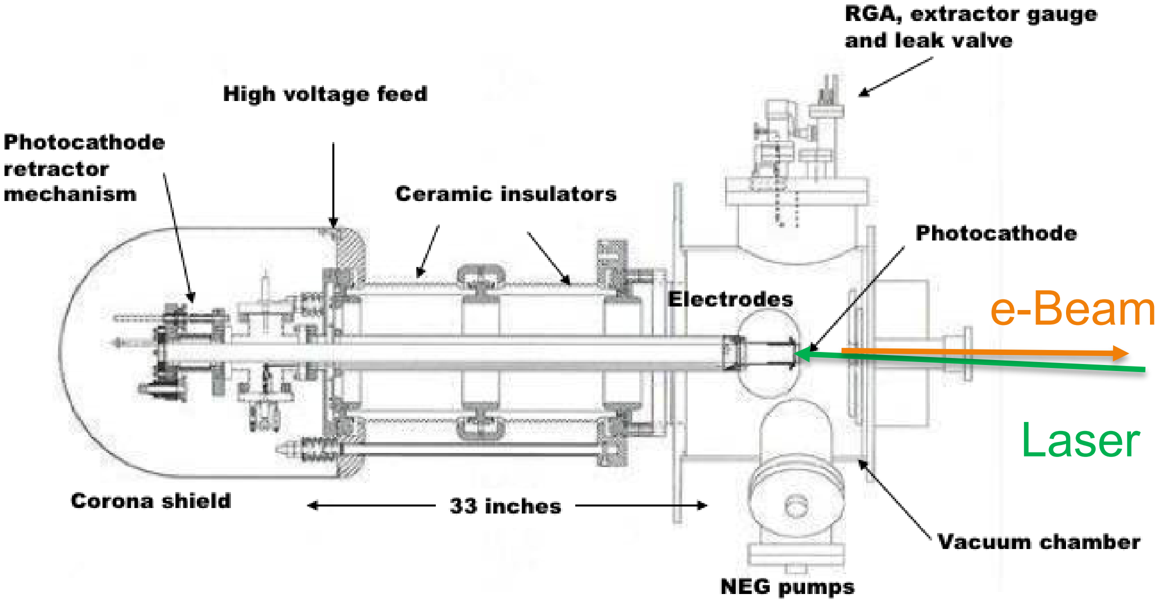

<u>Injector for JLAB FEL</u>
Design – DC
DC Voltage – 350 kV
Cathode material – GaAs
Electron beam current – 10 mA
Beam structure – 1.4 MHz to 75 MHz, pulsed or CW
Charge-per-bunch: 135 pC
No polarization

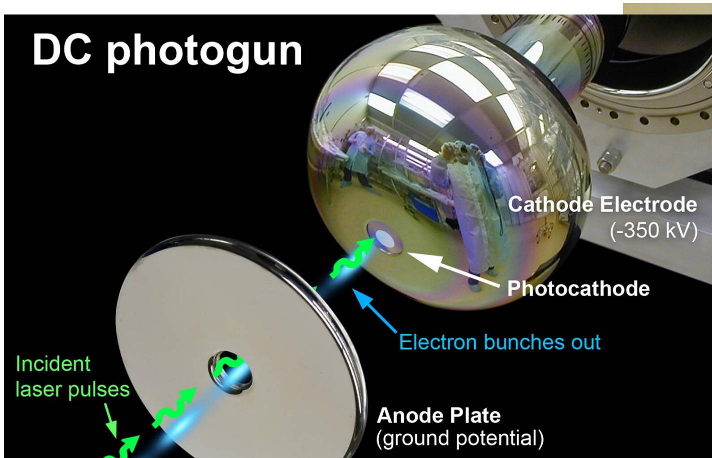

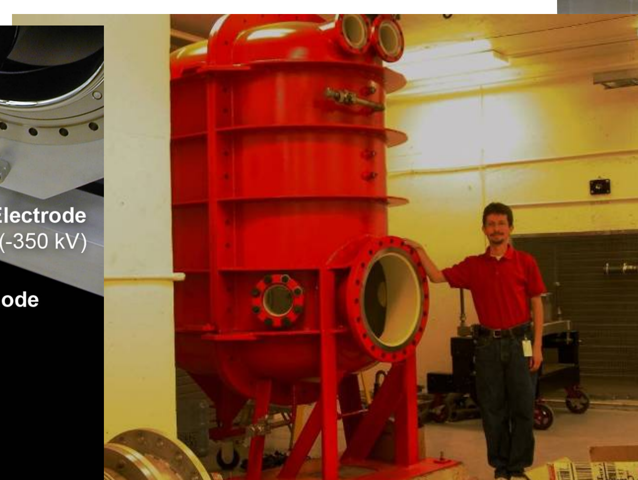

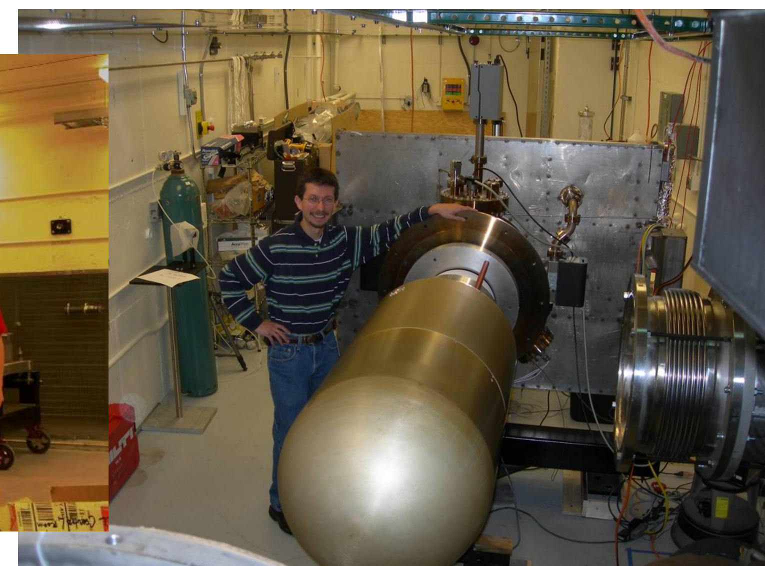

Warm RF Photo Guns
Suitable for Pulsed Operations

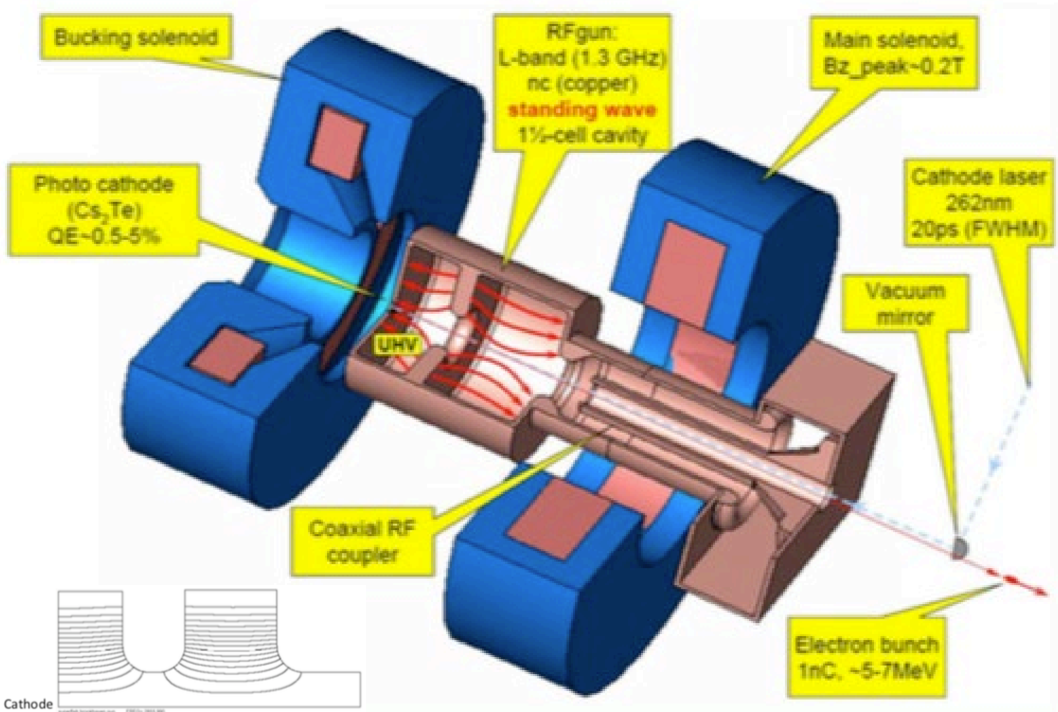

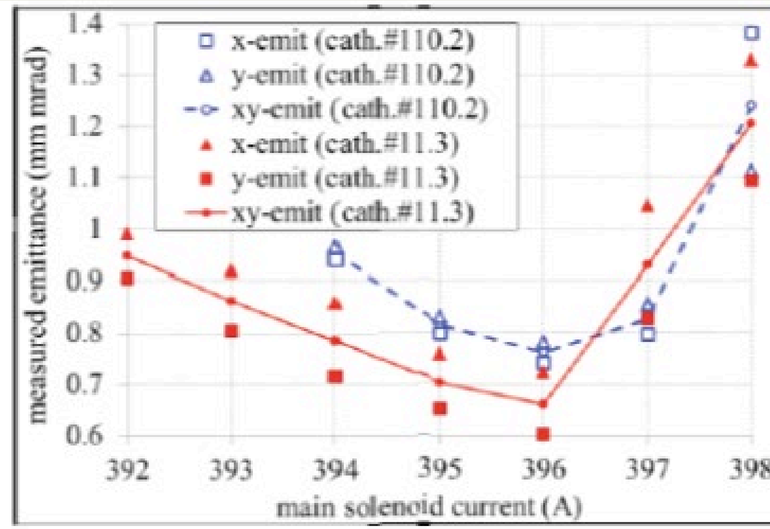

Parameters	FLASH	European XFEL
max. RF repetition rate	10 Hz	10 Hz
max. train length	800 µs	600 µs
bunch spacing	1 µs	0.2 – 1 µs

PITZ L-band Gun
Frequency = 1,300 MHz
Gradient = up to 60 MV/m
Exit energy = 6.5 MeV
Cs_2Te photocathode
800 bunches per macropulse
Normalized rms emittance
1 nC 0.70 µm
0.1 nC 0.21 µm

Low Frequency Warm Photo Gun for LCLS-II Optimized for CW Applications

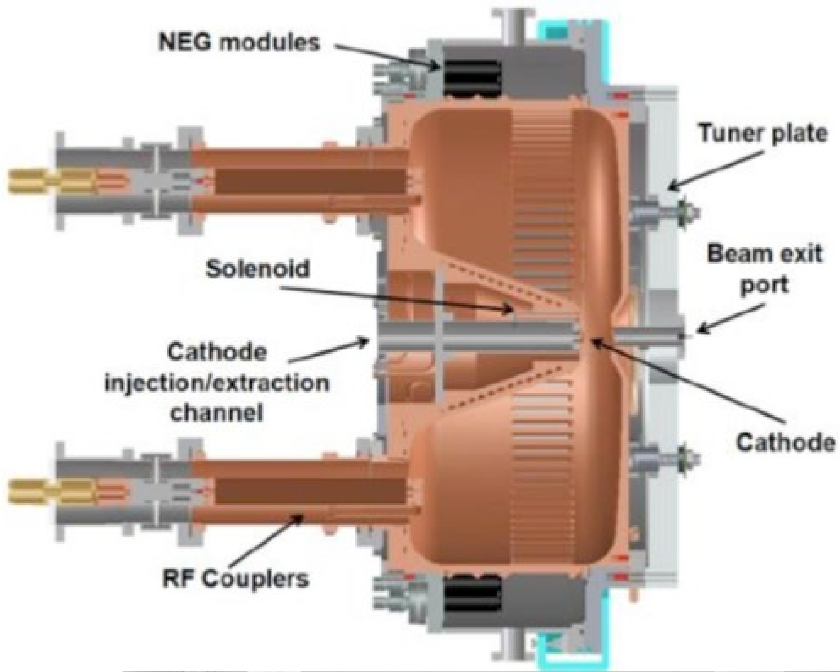

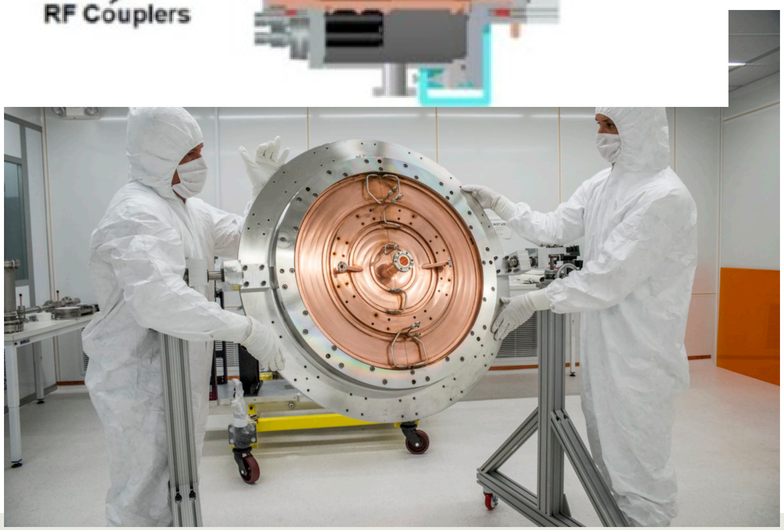

Frequency	186 MHz
Operation mode	CW
Gap voltage	750 kV
Field at the cathode	19.47 MV/m
Q_0 (ideal copper)	30887
Shunt impedance	6.5 MΩ
RF Power	100 kW
Stored energy	2.3 J
Peak surface field	24.1 MV/m
Peak wall power density	25.0 W/cm^2
Accelerating gap	4 cm
Diameter/Length	69.4/35.0 cm
Operating pressure	~ 10^{-11} Torr

SRF Photo Gun Is Most Promising CW Design Most Difficult As Well

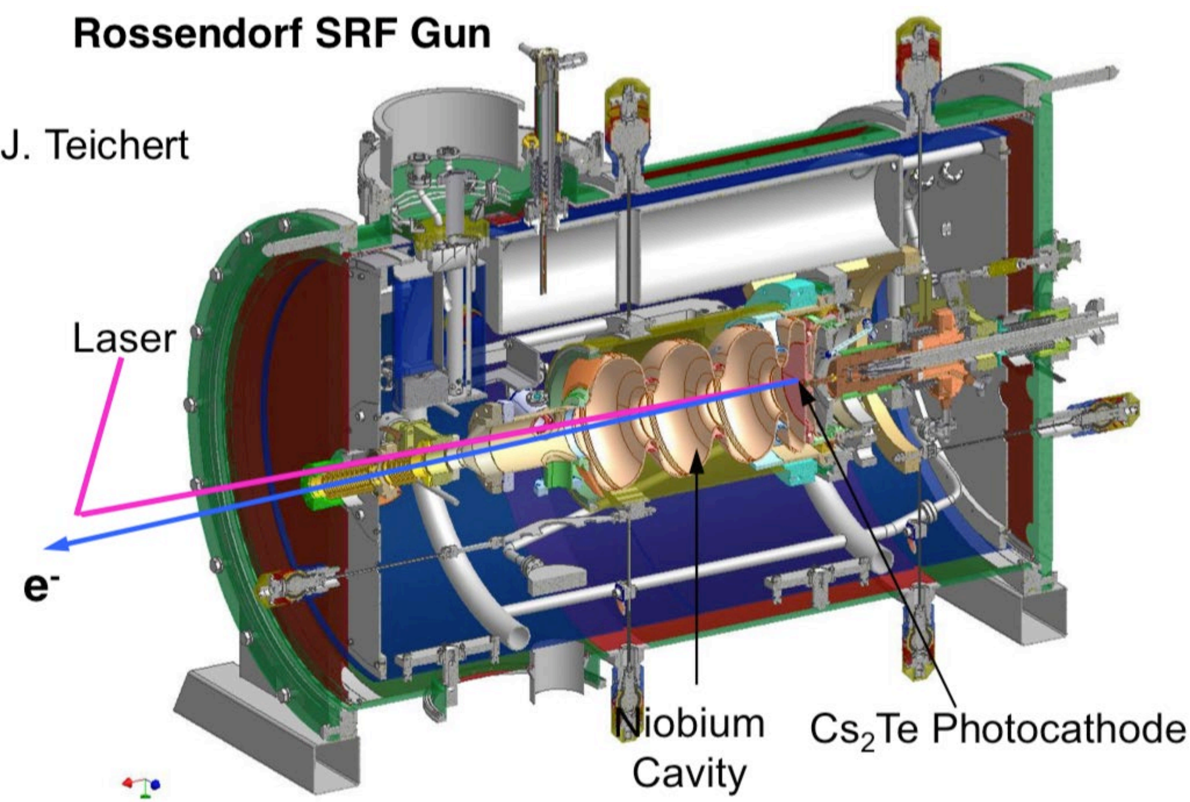

Location: Rossendorf, Germany

Design energy – 9 MeV
Achieved energy - 7 MeV
Status – Operational

SRF Guns have multiple issues when operated with a Photocathode:

- Multipacting in cathode area
- Cathode cooling
- Contamination during Cathode exchange

Collective Effects in Electron Linacs

Space Charge In Electron Linacs
Quickly Reduces with Energy, Important In Injectors

Uniformly charged beam with test particle shifted vertically and moving with beam

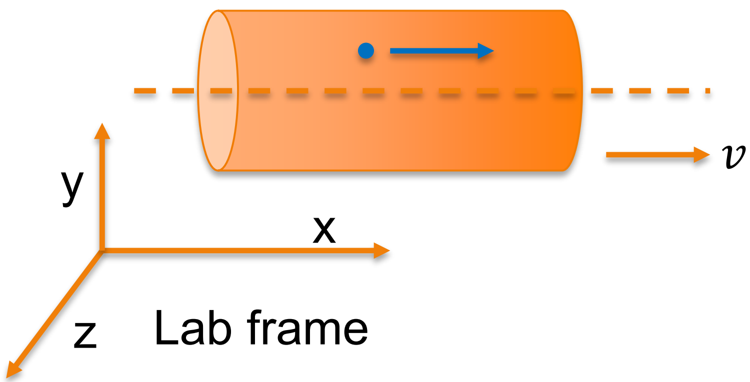

$$E'_x = E_x \qquad B'_x = B_x$$
$$E'_y = \gamma(E_x - {}^{v}/_{c}\, B_z) \qquad B'_y = \gamma(B_x + {}^{v}/_{c}\, E_z)$$
$$E'_z = \gamma(E_z + {}^{v}/_{c}\, B_y) \qquad B'_z = \gamma(B_z - {}^{v}/_{c}\, E_y)$$

$$E_y = \gamma E'_y \qquad B_y = -\gamma\, {}^{v}/_{c}\, E'_z$$
$$E_z = \gamma E'_z \qquad B_z = \gamma\, {}^{v}/_{c}\, E'_y$$

$$\rho' = \frac{\rho}{\gamma}$$

$$div E' = 4\pi\rho' \quad \Rightarrow \quad E'_y = 2\pi\rho' y$$

$$\boldsymbol{F_y = e\left(E_y - \frac{v}{c}B_z\right) = e\gamma E'_y\left(1 - \frac{v^2}{c^2}\right) = \frac{2\pi e\rho}{\gamma^2}y}$$

Space charge force quickly reduces with beam energy

Space charge is frequently unimportant beyond an injector energy of a few MeV

Space Charge in Injectors and Emittance Degradation

Transverse Space Charge force and defocusing are not constant along the bunch
This causes degradation of total "projected" emittance of the bunch

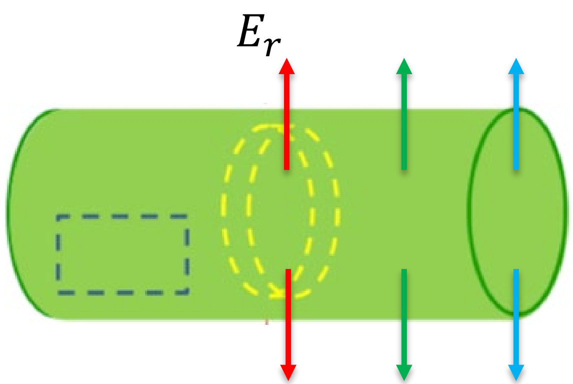

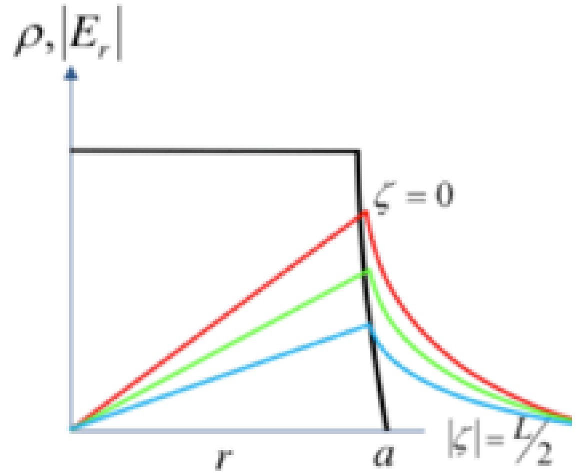

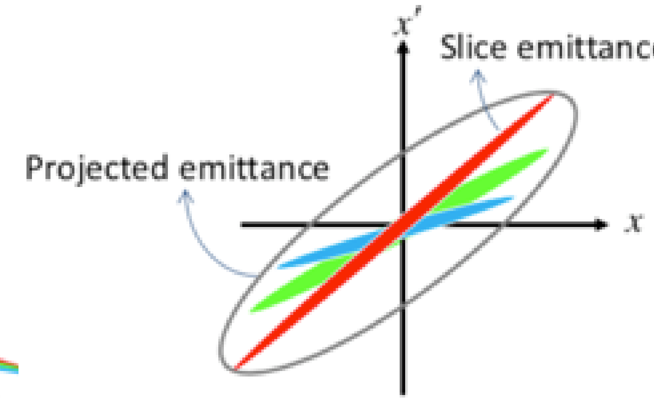

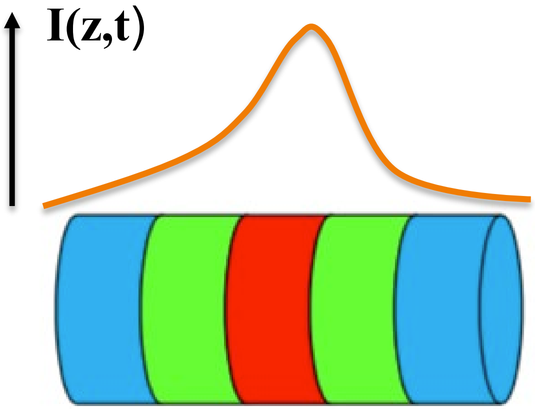

Initial bunch with 5 slices

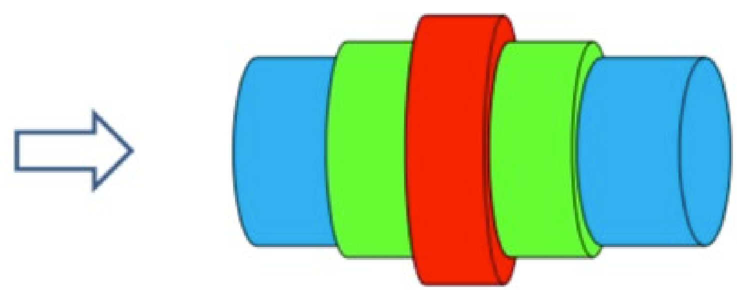

Different slices expand radially at different rates

Emittance Compensation Method

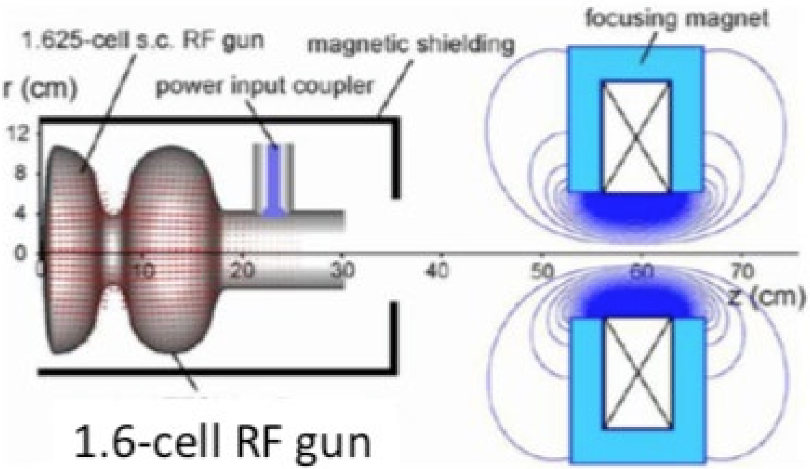

Ref. Carlsten, Serafini, and Rosenzweig

The idea is to use a solenoid magnet to flip the trace-space ellipses and let them move in x-x’ space until the slices are aligned to form smaller projected emittance.

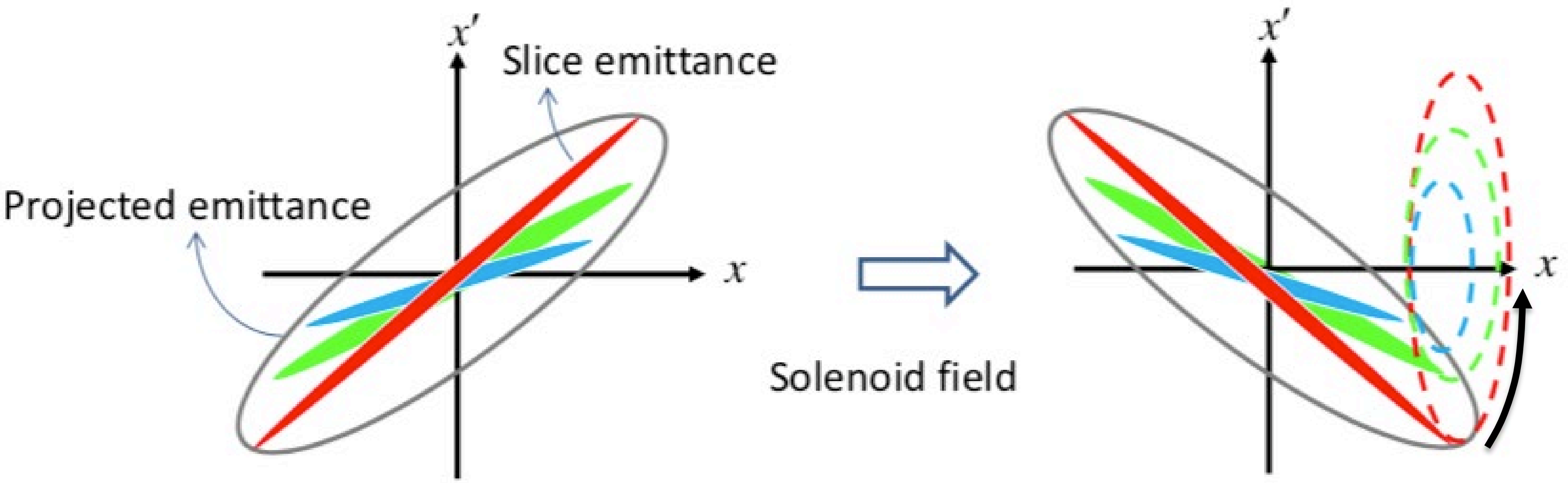

Emittance Compensation in Practice

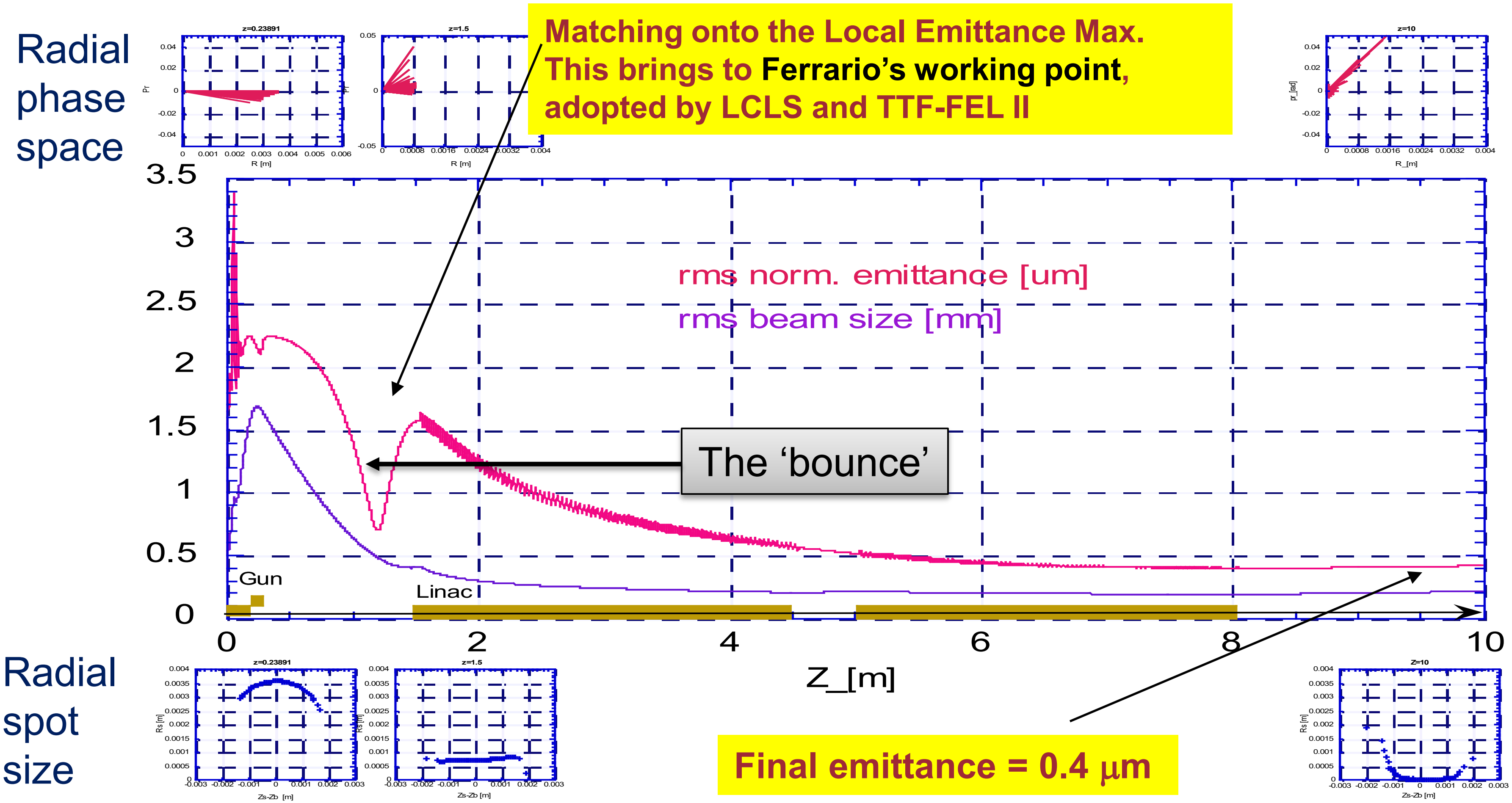

S-band photoinjector up to 150 MeV, HOMDYN simulation

(RF Gun + 2 Traveling Wave Structures)

Courtesy L. Serafini

Q=1nC, L=10ps, R=1 mm, E_{peak}=140 MV/m, TW E_{acc} = 25 MV/m

Emittance Exchange

Low energy electron beams have asymmetric emittances due to fundamental processes during emission. Longitudinal emittance << Transverse emittance

Longitudinal → Transverse

Beams produced in photoinjectors (several mm to cm in transverse size at cathode, short pulses ~1-10 ps, low longitudinal emittance growth in low charge (10s-100s pC), 'explosive' blow out in nC charge) typically have very small longitudinal emittances (from low energy spread) and larger transverse emittances, often differing by orders of magnitude.

Transverse → Transverse

Other sources of large emittance ratios occurs in magnetized sources (ie. a solenoid magnetic field threads the cathode). Busch's Theorem and canonical angular momentum contribute to large (correlated) emittance values. The large correlations in position/angular momentum can be 'unraveled' and reapportioned between transverse emittance planes.

→ Flat beams with large ratio between horizontal and vertical emittances.

Repartitioning beam emittances aids in reducing overall effects of instabilities and can maintain high beam brightness.

Demonstration of Flat Beam Adapter

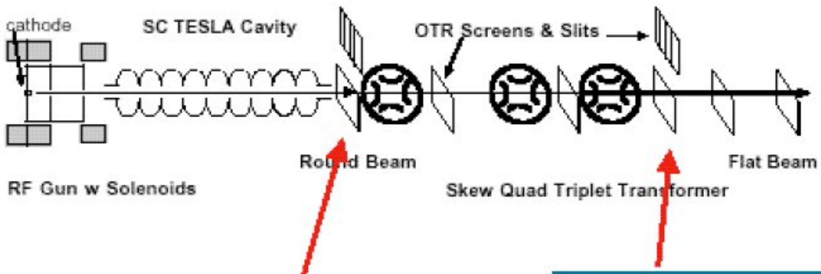

FNPL facility

- Original beamline modifications designed for demonstration of flat beam Adapter.
- Modified extensively in June 2003 to simplify Adapter lattice and beam transport.

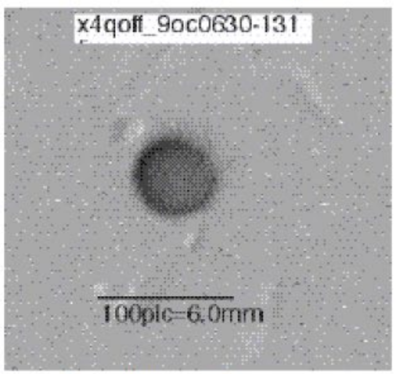

Round beam image on fluorescent screen

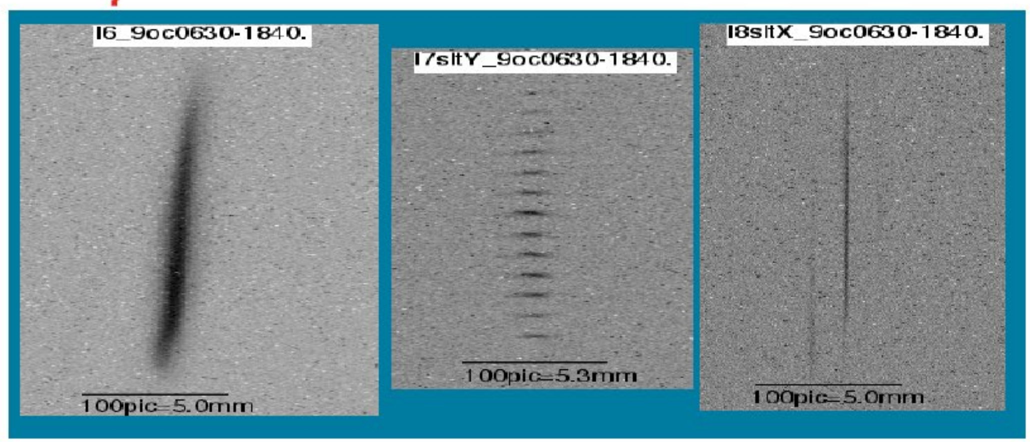

Flat beam image on fluorescent screen

Beam image through slits for emittance measurement

Horizontal emittance ~ 0.9 mm-mrad @ 1nC (Vertical emittance ~ 45 mm-mrad).
Horizontal measurement resolution-limited by finite CCD pixel size (~1 μm).

Longitudinal-Transverse Emittance Exchange

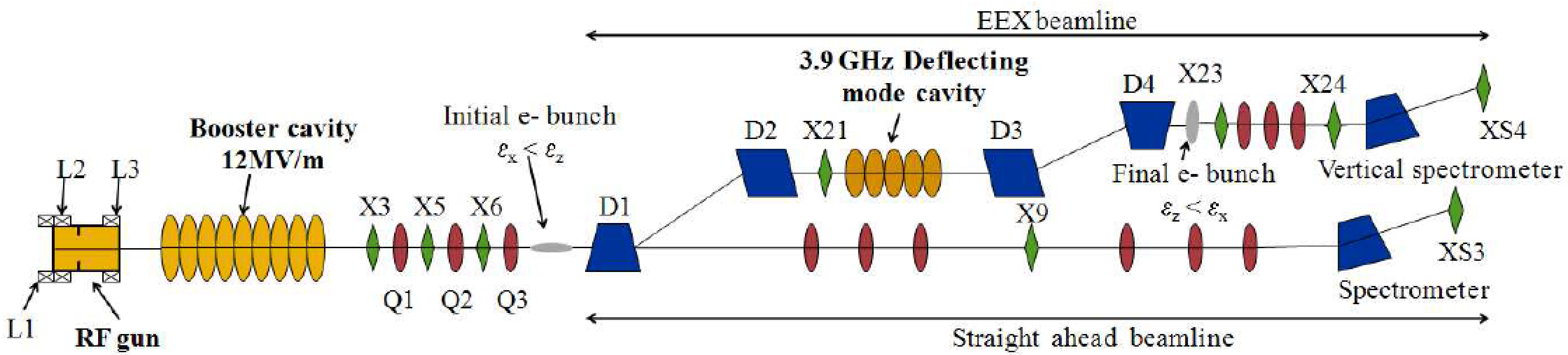

Incoming

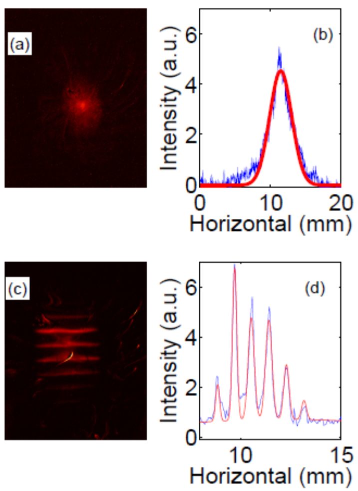

Outgoing

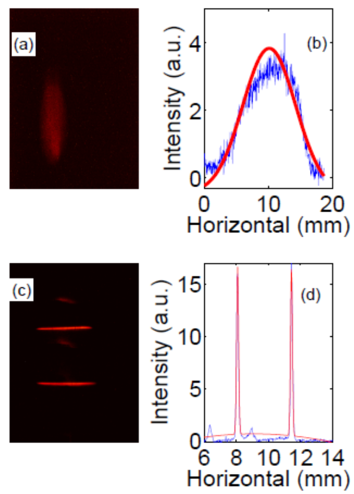

Transverse emittance measurements

Figure 2: Incoming transverse emittance images. Beam profile image taken at X3 OTR screen (a) with Gaussian fits to the x-projection (b) and the slit images taken on a YAG:Ce crystal screen located at X6 (c) with respective Gaussian fits (d). Images are rotated 90°.

Figure 3: Outgoing transverse emittance images. Beam profile image taken at X23 OTR screen (a) with Gaussian fits to the x-projection (b) and the slit images taken on a YAG:Ce crystal screen located at X24 (c) with respective Gaussian fits (d). Images are rotated 90°.

	Simulated		Measured	
	In	Out	In	Out
ϵ_x	3.7	18.7	3.7 ± 0.1	13.9 ± 1.2
ϵ_y	3.3	3.3	3.3 ± 0.1	4.7 ± 0.4
ϵ_z	16.2	9.2	16.2 ± 1.5	7.7 ± 2.0

DEMONSTRATION OF TRANSVERSE-TO-LONGITUDINAL EMITTANCE EXCHANGE AT THE FERMILAB PHOTOINJECTOR *

A. Johnson[1], J. Ruan[1], H. Edwards[1], T. Koeth [1], A. Lumpkin[1], P. Piot[2,3], J. Santucci[1], Y.-E Sun[2], R. Thurman-Keup[1]
[1] Accelerator Division, Fermi National Accelerator Laboratory, Batavia, IL 60510, USA
[2] Accelerator Physics Center, Fermi National Accelerator Laboratory, Batavia, IL 60510, USA
[3] Department of Physics, Northern Illinois University, DeKalb, IL 60115

Wake Fields
Electromagnetic Reciprocity

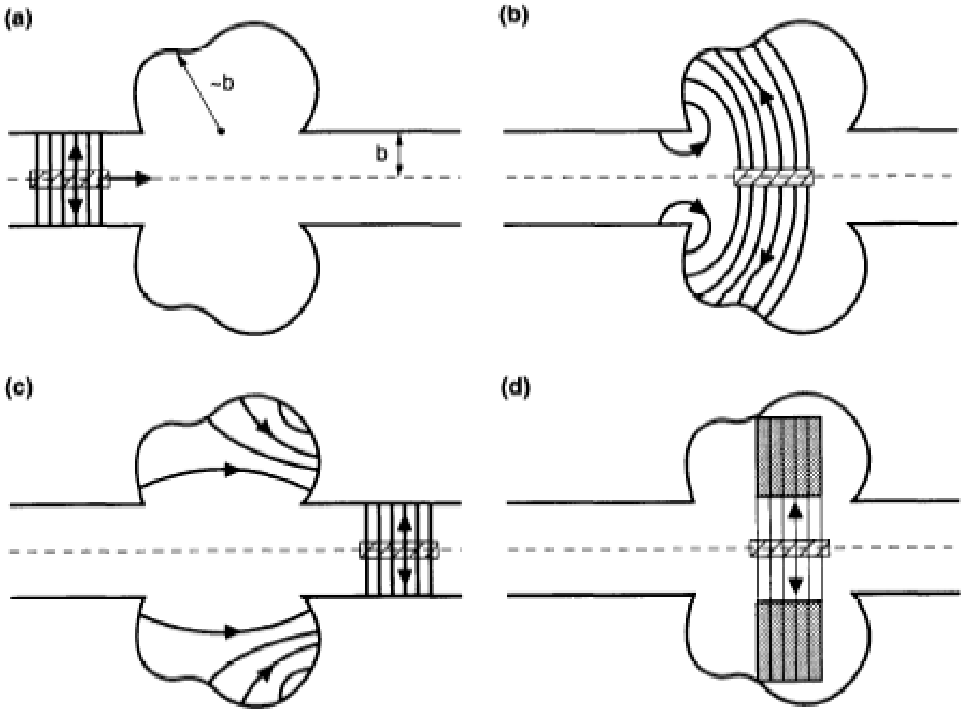

SLAC–PUB–4547
SLAC/AP–66
January 1989
(A/AP)

INTRODUCTION TO WAKEFIELDS AND WAKE POTENTIALS*

P. B. Wilson

Stanford Linear Accelerator Center,
Stanford University, Stanford, California 94309

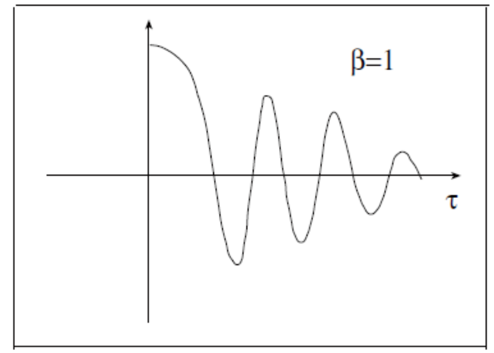

Fields induced by ultra-relativistic particles in inhomogeneities can produce forces affecting particles of the test bunch and following bunches. These fields are called wake-fields. Finite resistivity of the surface of the vacuum chamber and machining marks can induce wake fields as well. These fields and forces depend on the charge of bunches, displacement of bunches, and geometry of inhomogeneities.

Wakefunctions and Impedances

see Chao, ‘Physics of Collective Beam Instabilities In High Energy Accelerators”

- Integrated forces – impulses – from one beam component to another
- Test construction is driven by cos$m\theta$ charge ring to test charge, e
- Ultrarelativistic approximation. Axial symmetry (on average) assumed. z=s-ct

$$F_{\parallel} = eE_s$$
$$F_{\theta} = e(E_{\theta} + B_r)$$
$$F_r = e(E_r - B_{\theta})$$

→

$$\int_{-L/2}^{L/2} ds\overrightarrow{F_{\perp}} = -eI_m W_m(z) m r^{m-1}\left(\hat{r}\cos m\theta - \hat{\theta}\sin m\theta\right)$$
$$\int_{-L/2}^{L/2} dsF_{\parallel} = -eI_m W_m'(z) r^m \cos m\theta$$
$$\int_{-L/2}^{L/2} dsB_s = eI_m W_m'(z) r^m \sin m\theta$$

Current rings and point charges

$$[W_m] = length^{-2m}$$

Table 2.2. The longitudinal and transverse wake potentials $\int_{-L/2}^{L/2} ds\, F_{\parallel}$ and $\int_{-L/2}^{L/2} ds\, \vec{F}_{\perp}$ seen by a test charge e a distance $|z|$ behind a beam which possesses an mth moment.

m	Distribution Moments of Beam	Longitudinal Wake Potential	Transverse Wake Potential
0	q	$-eqW_0'(z)$	0
1	$q\langle x\rangle$	$-eq\langle x\rangle xW_1'(z)$	$-eq\langle x\rangle W_1(z)\hat{x}$
	$q\langle y\rangle$	$-eq\langle y\rangle yW_1'(z)$	$-eq\langle y\rangle W_1(z)\hat{y}$
2	$q\langle x^2 - y^2\rangle$	$-eq\langle x^2 - y^2\rangle(x^2 - y^2)W_2'(z)$	$-2eq\langle x^2 - y^2\rangle W_2(z)(x\hat{x} - y\hat{y})$
	$q\langle 2xy\rangle$	$-eq\langle 2xy\rangle 2xyW_2'(z)$	$-2eq\langle 2xy\rangle W_2(z)(y\hat{x} + x\hat{y})$
3	$q\langle x^3 - 3xy^2\rangle$	$-eq\langle x^3 - 3xy^2\rangle(x^3 - 3xy^2)W_3'(z)$	$-3eq\langle x^3 - 3xy^2\rangle W_3(z) \times[(x^2 - y^2)\hat{x} - 2xy\hat{y}]$
	$q\langle 3x^2y - y^3\rangle$	$-eq\langle 3x^2y - y^3\rangle(3x^2y - y^3)W_3'(z)$	$-3eq\langle 3x^2y - y^3\rangle W_3(z) \times[2xy\hat{x} + (x^2 - y^2)\hat{y}]$

$$J_0(s,t) = \widehat{J_0}e^{-i(ks-\omega t)}$$
$$V(s,t) = -J_0(s,t)Z_0^{\parallel}(\omega)$$

$$Z_m^{\parallel}(\omega) = \int_{-\infty}^{\infty}\frac{dz}{c}e^{-i\omega z/c}W_m'(z)$$
$$Z_m^{\perp}(\omega) = i\int_{-\infty}^{\infty}\frac{dz}{c}e^{-i\omega z/c}W_m(z)$$

Sinusoidal currents

↓

Lead to Impedances

Effect of Wake Fields on Beam

- Short Range / High Frequency Wakes (within a single bunch)
  - Energy loss
  - Energy spread, tail loses more energy than head
  - Tail deflection and emittance growth
- Long Range Wakes (multi-bunch or multi-pass, below pipe cut off)
  - Energy deposition in linac vacuum chamber
  - Energy spread from bunch to bunch
  - Transverse Beam Instabilities – bunches get deflected by wakes. The mechanism can lead to amplification of the wake fields if a positive feedback mechanism exist
- Simulation of Wake Fields
  - Several Programs exist to simulate wake fields
  - ABCI, TBCI, CST MWS, and more

M. Venturini and J. Qiang, PRSTAB 18, 054401 (2015)

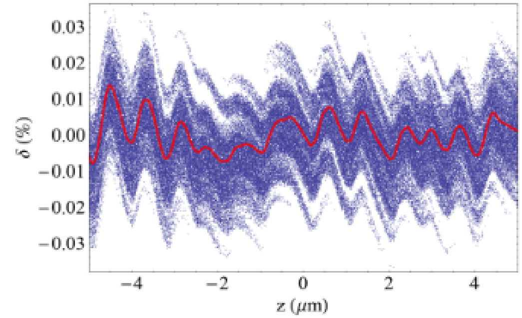

FIG. 3. Longitudinal phase space of the beam core at the entrance of DL1. The red curve is the slice centroid energy. The apparent ~1 μm energy modulation is the result of LSC during acceleration and transport following the second bunch compressor, placed about 700 m upstream of DL1.

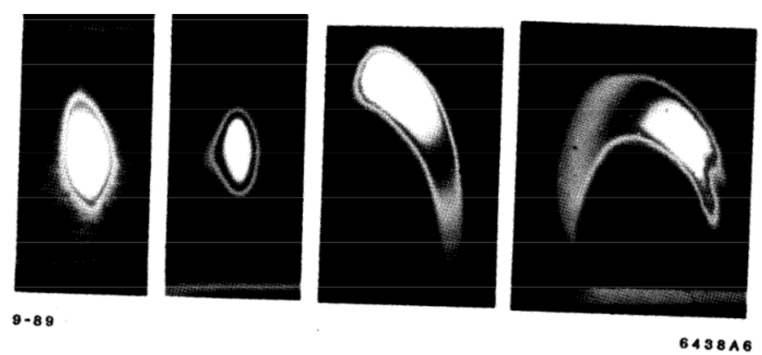

Figure 12 Images of an electron bunch on a profile monitor at 47 GeV showing wakefield growth with increasing oscillation amplitudes (136). The images from left to right are for a well-steered beam, a 0.2 mm oscillation, 0.5 mm oscillation, and a 1.0 mm oscillation, respectively. The beam intensity is 2 X 10^{10} electrons. The core sizes σ_x and σ_y are about 120 μm.

J.T. Seeman, 1991

Loss factor and kick factor

- Parasitic losses are parameterized by $\Delta E = -\kappa_{||} q^2$, where $\kappa_{||}$ is the ***loss factor*** (typical units of V/pC) and q is the bunch charge.
- Losses are highly dependent on bunch shape through the spectral power density $h(\omega,\sigma) = \tilde{\lambda}(\omega)\tilde{\lambda}^*(\omega)$ for line charge λ with rms length σ
- In terms of the wake and impedance functions

$$\kappa_{||}(\sigma) = \frac{1}{2\pi}\int_{-\infty}^{\infty} d\omega Z_{||}(\omega) h(\omega,\sigma) \qquad \kappa_{||} = \int_{-\infty}^{\infty} d\tau W_{||}(\tau)\lambda(\tau)$$

- ***Kick factors*** (V/pC-m) are related to transverse impulses from dipole modes

$$\kappa_{\perp}(\sigma) = \frac{1}{2\pi}\int_{-\infty}^{\infty} d\omega Z_{\perp}(\omega) h(\omega,\sigma) = \int_{-\infty}^{\infty} d\tau W_{\perp}(\tau)\lambda(\tau)$$

Loss factor examples

Case	$\kappa_{\|\|}(\sigma) \approx$	$\kappa_{\perp}(\sigma) \approx$
High-Q cavity mode (Q>10)	$\frac{\omega_r R_s}{2Q_r} e^{-\omega_r^2 \sigma^2}$	$\frac{\omega_r R_\perp}{4Q_r'}[w(\omega_1 \sigma) - w(\omega_2 \sigma)]$ Where $\omega_{1,2} = \frac{\omega_r}{Q_r}[-i/2 \pm Q_r'], \quad {Q_r'}^2 = Q_r^2 - \frac{1}{4}$ $\mathrm{w(z) = erfc(z)}$
Short bunches, $\omega_r \sigma \ll 1$	$\frac{\omega_r R_s}{2Q_r \pi}\left[1 - \frac{2}{\pi}\frac{\omega_r \sigma}{Q_r}\right]$	$\frac{\omega_r R_\perp}{Q_r}\frac{\omega_r \sigma}{\sqrt{\pi}}$
Low-Q cavity and long bunches	$\frac{R_s}{4\sqrt{\pi} Q^2 \omega_r^2 \sigma^3}$	$\frac{R_\perp}{Q_r}\frac{1}{2\sqrt{\pi}\sigma}$

Simulation of Wake Fields
Example: BNL 5 –cell cavity

F = 703.75 MHz
δE = 20 MeV
$Q_0 \sim 10^{10}$
$Q_{HOM} \sim 10^3$

Build: AES
Processed: JLAB

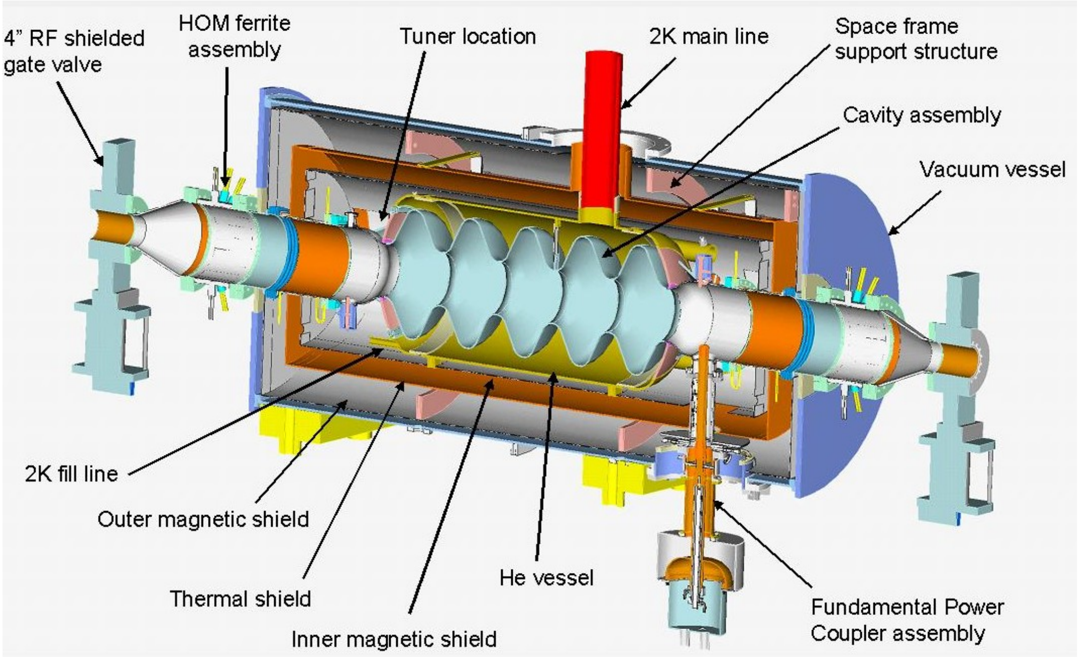

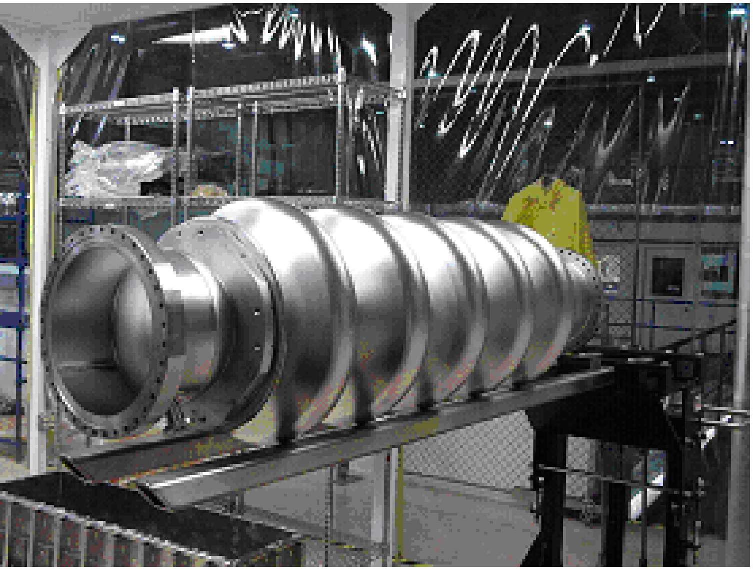

The 5-cell cavity was specifically designed for high current, high bunch charge applications such as eRHIC and a high energy electron cooler. The loss factor of the cavity was minimized. The number of cells was limited to 5 to avoid HOM trapping. Additionally, HOM power is effectively evacuated from the cavity via an enlarged beam pipe piece.

5 cell cavity Wake Fields Single Bunch Effects were simulated with ABCI

Integrated loss factor as a function of frequency (σ_z=1cm)

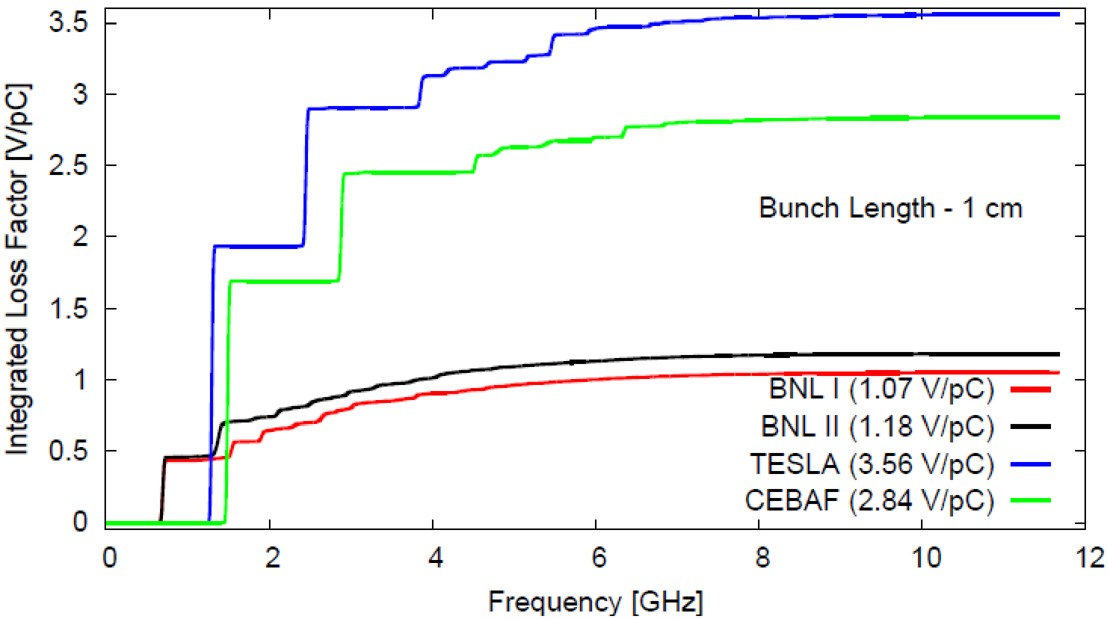

R. Calaga,
Ph.D. Dissertation

Generated power: $P_{av} \approx k_{\|} q_b^2 f_b$

For 5 nC and 10 MHz, $P_{av} \approx 300$ W
For 1.4 nC and 700 MHz, $P_{av} \approx 700$ W

A large portion of the power is generated in HOMs.

Energy spread due to short range wakes is small: $$\frac{\delta E}{E} \approx 2k_{\|} \frac{q_b}{\delta E_{acc}} \approx 5 \cdot 10^{-4}$$

Beam Breakup (BBU) Instabilities

- Generated by beam interaction with discrete or distributed impedances
- For a linear system of thin resonator cavities, in an axisymmetric beamline, the advance of the beam centroid advances between cavities as

$$\begin{pmatrix} r \\ p_r \end{pmatrix}_n = \begin{pmatrix} \cos\theta & \frac{1}{\omega}\sin\theta \\ -\omega\sin\theta & \cos\theta \end{pmatrix} \begin{pmatrix} 1 & 0 \\ R & 1 \end{pmatrix} \begin{pmatrix} r \\ p_r \end{pmatrix}_{n-1}$$

- Here θ is the betatron advance between cavities, ω is the betatron frequency, and R is the integral operator for the interaction between cavity and beam ('kick' or wake)

$$Rr_n = \frac{e\omega^2 Z_\perp}{c^2 Q} \int dt' e^{-[\omega(t-t')/2Q]} I(t') r_n(t') \sin[\omega(t-t')]$$

- This instability is quite severe and limits the maximum transmitted beam intensity, if uncorrected.

BBU Impedances and Wakes

- Discussed in Chao, 'Physics of Collective Beam Instabilities In High Energy Accelerators"
- For dipole modes and treating the beam as a uniform disk (radius *a*)

$$Z_m^{\parallel}(\omega) = \frac{R_s}{1 + iQ\left(\frac{\omega_R}{\omega} - \frac{\omega}{\omega_R}\right)}$$

$$Z_m^{\perp}(\omega) = \frac{c}{\omega} Z_0^{\parallel}(\omega) = \frac{c}{\omega}\frac{R_s}{1 + iQ\left(\frac{\omega_R}{\omega} - \frac{\omega}{\omega_R}\right)}$$

- The transverse wake function is

$$W_m(z) = \frac{cR_s\omega_R}{Q\bar{\omega}} e^{\alpha z/c} \sin\frac{\bar{\omega} z}{c},$$

$$\alpha = \frac{\omega_R}{2Q}, \bar{\omega} = \sqrt{\omega^2 - \alpha^2}$$

$$z < 0 \ (ie. trailing\ particles)$$

Single mode, long-range wake

For an S-band linac with Gaussian bunches of length σ_z = 1.5 mm, summing up the modes and fitting produces (K. Bane, et al, DESY M97-02, 1997)

$$w_\perp(s) = 4.1\left[1 - \left(1 + 1.15\, s^{1/2}\right)e^{-1.15 s^{1/2}}\right] \text{kV/pC/mm}^2$$

and the transverse wake potential of the bunch is given by convolution with the longitudinal distribution $\lambda(s)$, *s* in mm

$$W_\perp(s) = \int_{-\infty}^{s} \lambda(s') w_\perp(s - s') ds'$$

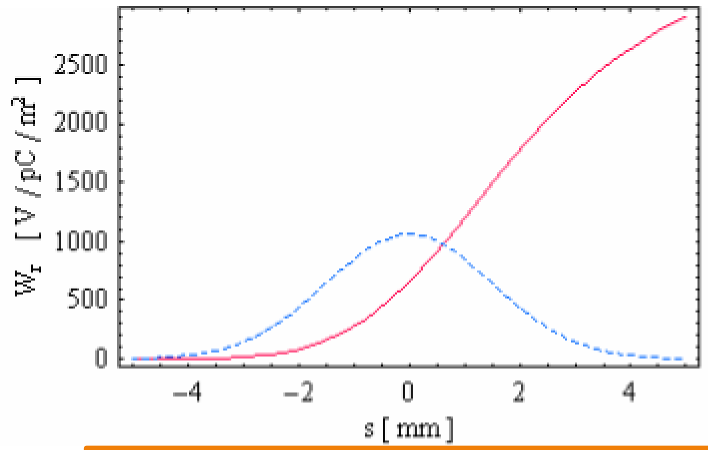

Many modes, short-range wake

Dipole BBU With Acceleration
Two Particle Model

- Consider two beam particles with transverse offsets, y_1 and y_2 , separated by z<0, in an acceleration channel

  Particle 1: $\frac{d}{ds}\left[\gamma(s)\frac{dy_1}{ds}\right] + k_\beta^2\gamma(s)y_1 = 0$

  Particle 2: $\frac{d}{ds}\left[\gamma(s)\frac{dy_2}{ds}\right] + k_\beta^2\gamma(s)y_2 = -\frac{Nr_eW_1(z)}{2L}y_1$

  (Here, focusing strength is assumed to increase with energy)

- Assume uniform acceleration $\gamma(s) = \gamma_i(1+\alpha s)$
- Changing variables from s to $u = (1+\alpha s)$:

$$\frac{d^2y_1}{du^2} + \frac{1}{u}\frac{dy_1}{du} + \left(\frac{k_\beta}{\alpha}\right)^2 y_1 = 0 \quad \text{and}$$

$$\frac{d^2y_2}{du^2} + \frac{1}{u}\frac{dy_2}{du} + \left(\frac{k_\beta}{\alpha}\right)^2 y_2 = -\frac{Nr_eW_1(z)}{2\gamma_i\alpha^2Lu}y_1(u)$$

Here r_e is the classical electron radius ($2.81794\ 10^{-15}$ m), L is the cavity period, N is the number of electrons

Solutions for Two-Particle Model

- Solution for y_1: $y_1(u) = y_{init} \frac{\pi k_\beta}{2\alpha} \left[J_1\left(\frac{k_\beta}{\alpha}\right) N_0\left(\frac{k_\beta}{\alpha}u\right) - N_1\left(\frac{k_\beta}{\alpha}\right) J_0\left(\frac{k_\beta}{\alpha}u\right) \right]$

$$y_1(0) = y_{init} \quad y_1'(0) = 0 \text{ (initial conditions)}$$

- In asymptotic limit $\alpha \ll k_\beta$

$$y_1(u) \approx \frac{y_{init}}{\sqrt{1+\alpha s}} \cos k_\beta s \qquad y_2(u) \approx \frac{y_{init}}{\sqrt{1+\alpha s}} \left[\cos k_\beta s - \frac{N r_e W_1(z)}{4 k_\beta \gamma_i \alpha L} ln(1+\alpha s) \sin k_\beta s \right]$$

- In the **coasting beam limit:**

$$y_1(s) \approx y_{init} \cos k_\beta s \qquad y_2(s) \approx y_{init} \left[\cos k_\beta s - \frac{N r_e W_1(z)}{4 k_\beta \gamma L} s \sin k_\beta s \right]$$

BBU Suppression Methods

	Detune the resonance	Damp stored energy	Decrease initial seed	Other
Structure, Lattice	Vary dipole (HOM) frequencies	Couple HOM cavity power to loads; apply cavity mode feedback	Improve structure alignment	Strong focusing; adjust phase advance
Beam	Vary centroid beam energy; introduce betatron spread	Use feedback and kicker to reduce coherent oscillations	Inject beam on-axis; decrease slice perturbations	Increase slice energy spread (Phase mixed and Landau damping)

BBU Suppression
Development of RF Cavities with HOM Damping

- Design of multi-cell cavities with low-Q, low-R/Q HOMs seems to be the most reliable way to increase the BBU threshold in large-scale ERLs.The work is under way at BNL, JLAB, Cornell U…
- To provide adequate damping, HOM power must be effectively evacuated from a cavity and damped outside

Brookhaven National Lab
(Based on Cornell CESR Upgrade)

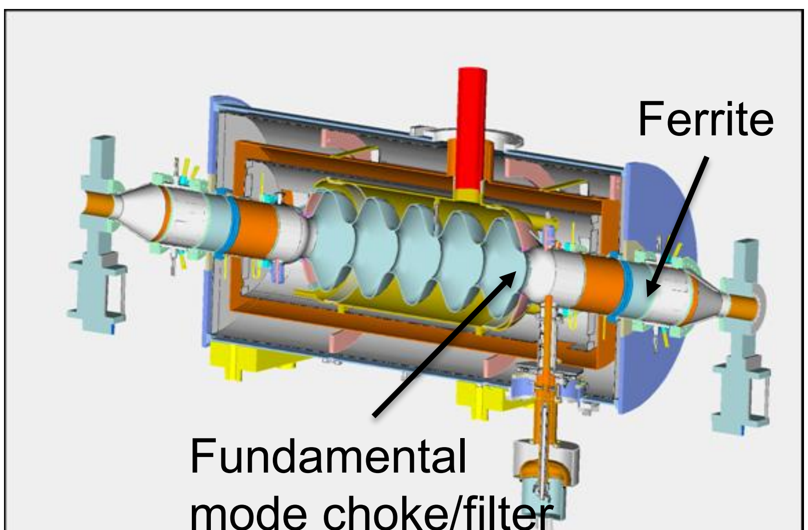

JLAB

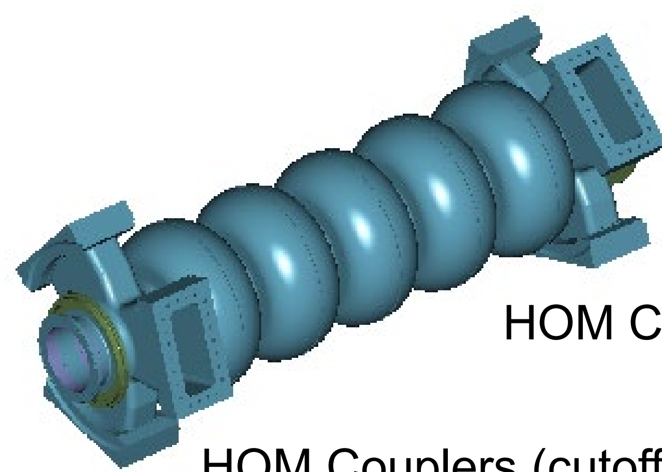

Beam Energy Spread

- Issue for linear colliders, where final focus spot size enlarges due to finite energy spread
- Critical issue for free electron lasers
- Beam current perturbations -> slice energy perturbations -> chromatic focusing and feedback gain to perturbation
  - Emittance growth in bunch compressors
  - Longitudinal space charge instability – ie. ‘microbunching’ instability

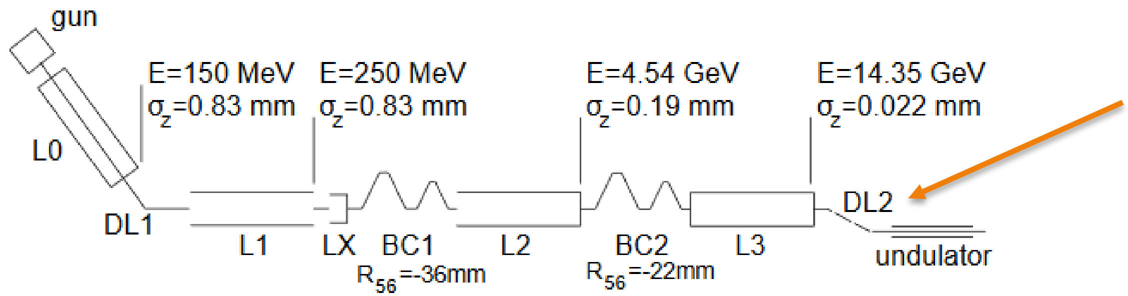

M. Borland et al. / Nuclear Instruments and Methods in Physics Research A 483 (2002) 268–272

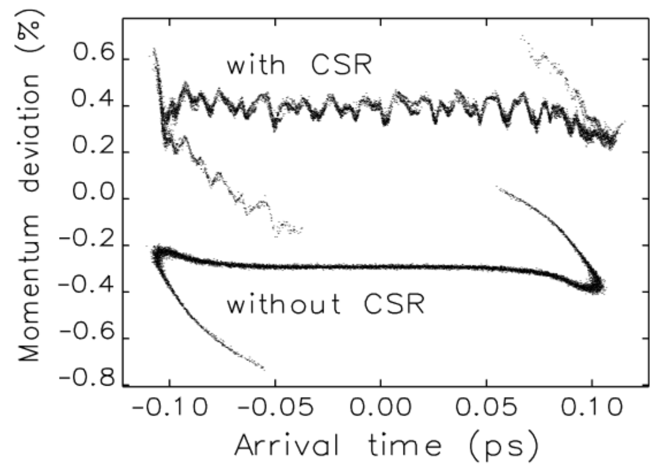

Laser Heater is Used to Combat Microbunching Instabilities

- RF photoinjectors produce beams with very small slice energy spread → can lead to coherent growth of instability and beam quality degradation
- A 'laser heater' increases local energy spread to create tune spread and buffer against instability growth in bunch compressors

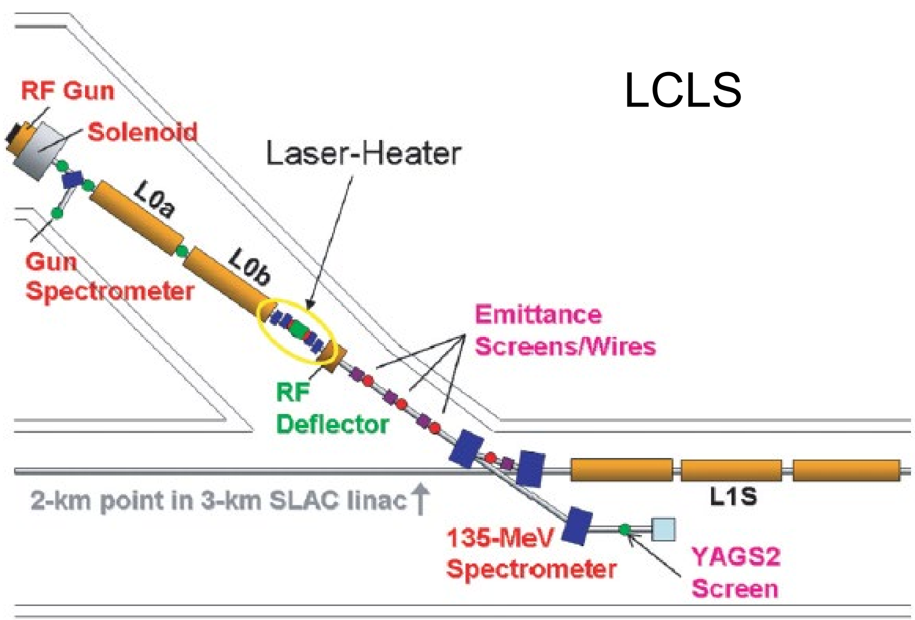

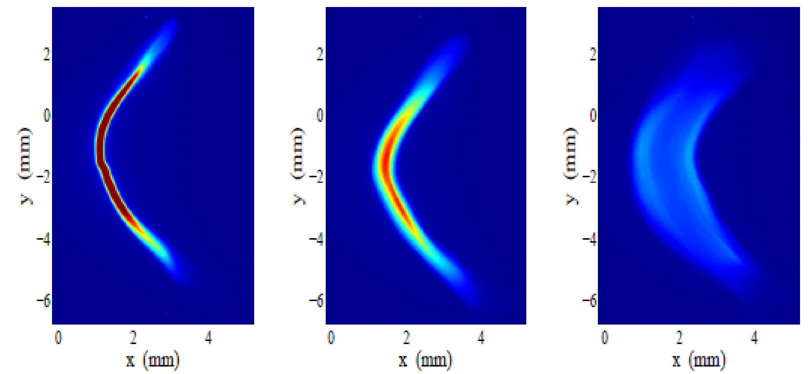

(a) no heating (b) nominal heating (c) maximum heating

Figure 4: Measured longitudinal phase space on "YAGS2" screen at 135 MeV with (a) laser heater off, (b) IR laser energy at 10 μJ, and (c) at 220 μJ.

Thank You!

Homework Problem

In the SLAC linac assume the following parameters:

a. What final deflection growth is expected for a 1 GeV coasting beam compared to the constantly accelerated beam? Define the total growth as

$$\Upsilon = y_{2,final}/y_{1,initial}$$

b. The SLAC beam has an RMS width of 20 μm. What is the acceptable beam offset at injection so that the final deflection (with acceleration) is less 10% of the beam size?

SLAC Linac Parameters	
Wake function/cavity, $W_1(z)$ [cm^{-2}]	-0.7*z[mm]
Cavity period, L [cm]	3.5
Accelerator length, L_0 [m]	3000
Beam intensity, N	$5\ 10^{10}$
Injection energy (1 GeV), $\gamma_{initial}$	2000
Final energy (50 GeV), γ_{final}	10^5
Normalized betatron wavenumber, k_β [m^{-1}]	0.06
Normalized acceleration gradient, α [m^{-1}]	0.016
Particle separation, z [mm]	1

Homework, cont'd

Next consider a spread in betatron wavenumbers along the beam generated by an energy spread and the lattice chromaticity, $\frac{\Delta k_\beta}{k_\beta} = \xi \frac{\Delta E}{E}$. The chromaticity, ξ, for a FODO lattice is $\xi = -\frac{2}{\mu}\tan\frac{\mu}{2}$, where μ is the betatron phase advance per FODO cell. Assume that $|\Delta k_\beta / k_\beta| \ll 1$.

c. Using the coasting beam equations of motion for y_1 and y_2, derive an expression for the trailing particle deflection in terms of k_β and Δk_β. Assume particle 1 is executing the betatron oscillation $y_1(s) \approx y_{init} \cos k_\beta s$ only. Show that for the trailing particle (at distance *z* from the leading particle)

$$y_2(s) = y_{init} \cos k_\beta s + \frac{A}{2k_\beta \Delta k_\beta} y_{init} \cos(k_\beta + \Delta k_\beta)s - \frac{A}{2k_\beta \Delta k_\beta} y_{init} \cos k_\beta s$$

$$= y_{init}\left[1 + \frac{A}{2k_\beta \Delta k_\beta}\right]\cos(k_\beta + \Delta k_\beta)s - y_{init}\left[\frac{A}{2k_\beta \Delta k_\beta}\right]\cos k_\beta s$$

where $A = \frac{N r_e W_1(z)}{2\gamma L}$

Homework, cont'd

d. What condition on the focusing spread ($\frac{\Delta k_\beta}{k_\beta}$) must hold between the leading and trailing particles so that they exhibit identical deflection? (This is the BNS condition, named for Balakin, Novokhatsky, and Smirnov). Express in terms of Υ, k_β, and L_0. Note that this expression remains true in the accelerated beam case, with suitable substitution of Υ.

e. For the SLAC case under acceleration, with $\mu = 90°$, and with particle separation z = -1 mm, what head-tail energy spread is required to satisfy the BNS condition? From where does this energy spread arise? Can it be controlled?

Effective Focusing

The effective focusing force depends on both applied magnetic field (plus any diamagnetic correction) as well as RF focusing in cavities.

$$k_{eff}^2 = \frac{\gamma''}{2\gamma\beta^2} + \left(\frac{qB_z}{\gamma\beta mc}\right)^2 \quad \rightarrow \quad \frac{\eta_{rf} + 2b^2}{8}\left(\frac{\gamma'}{\gamma}\right)^2$$

Here η_{rf} measures the combined influence of rf modes synchronous to the beam, while *b* is the ratio of magnetic to rf focusing.

For standing wave (SW) structures η_{rf} ~1, while travelling wave (TW) structures contribute less (by ~order of magnitude) to overall focusing.

Slice envelope orbits

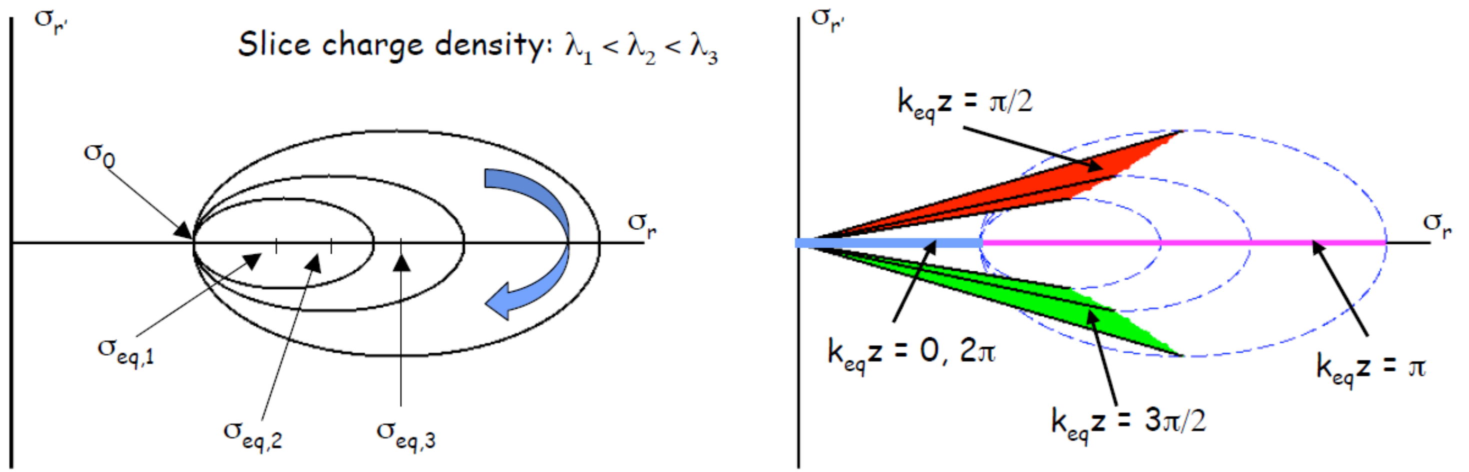

- Beam slices with varying charge density have different envelope radius equilibria.

- Slice envelopes undergo libration with identical periods.

- Projected emittance oscillates with slice envelopes.

Emittance oscillates around equilibrium

The linearized envelope equation admits the equilibrium wavenumber

$$k_{eq}^2 = k_{eff}^2 \left\{ 1 + \frac{2}{\left[1 + \left(1+\mu^2\right)^{1/2}\right]} + \frac{3\mu^2}{\left[1 + \left(1+\mu^2\right)^{1/2}\right]^2} \right\} \Rightarrow \begin{cases} 2k_{eff}^2 \ , & \mu^2 \to 0 \\ 4k_{eff}^2 \ , & \mu^2 \to \infty \end{cases}$$

Serafini & Rosenzweig (1997) showed that the emittance oscillates (for a coasting beam) along the beamline as

$$\varepsilon_{nr} \approx \frac{\gamma\beta}{2\sqrt{2}} k_{eq} \sigma_0 \sigma_{eq}\left(I_{peak}\right) \frac{\delta I_{rms}}{I_{peak}} \left|\sin\left(k_{eq} z\right)\right|$$

For small oscillations, k_{eq} is ~independent of local charge density.

Emittance compensation requires phase matching the oscillation in different areas of the beamline (RF gun, GTL drift, linac, etc.) with different focusing profiles.

Emittance compensation in round beam

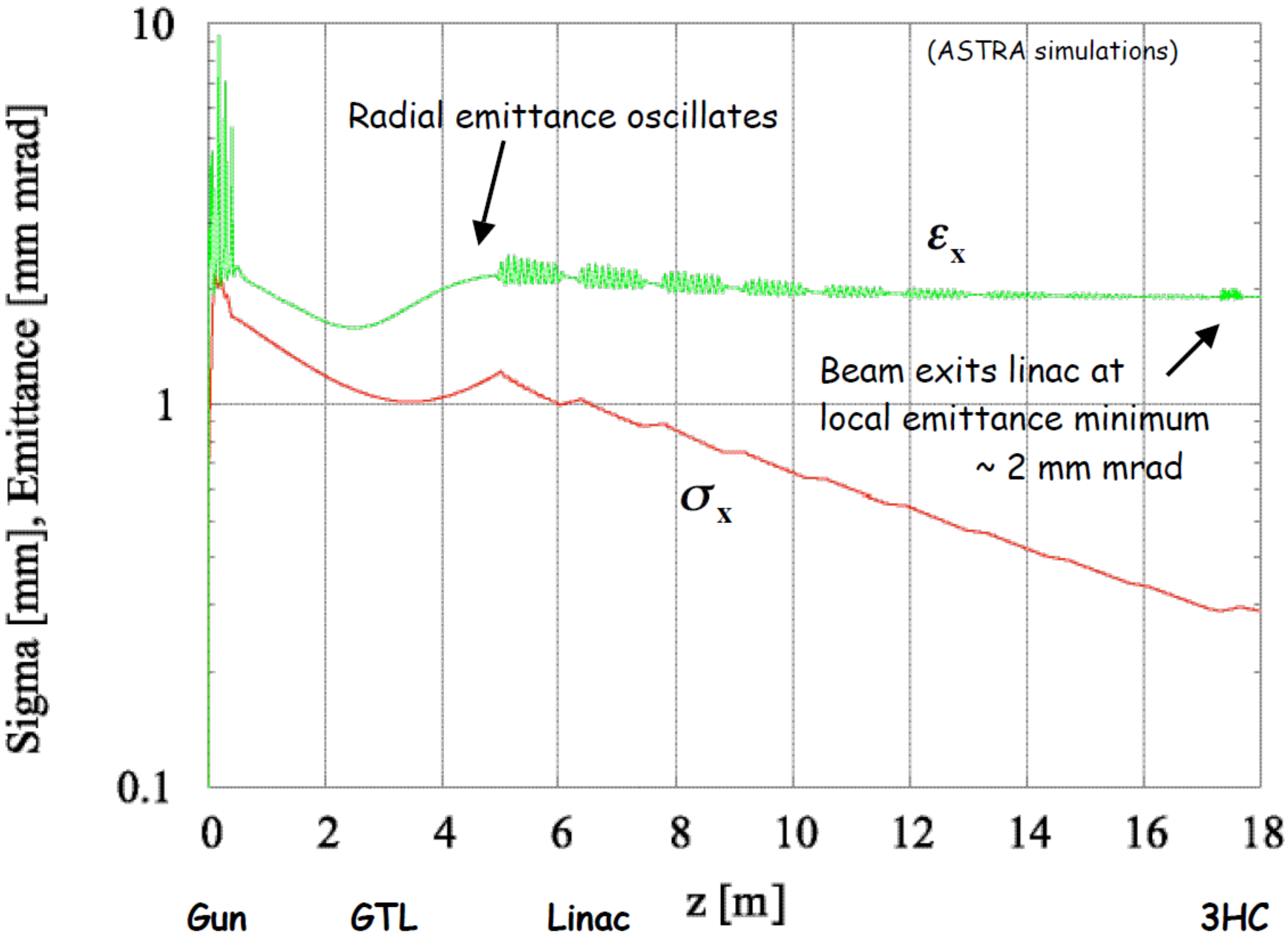

SW Linac Voltage [MV]

1. 9.0
2. 10.4
3. 13.1
4. 13.1
5. 13.1
6. 15.8
7. 15.8
8. 15.8

Normal modes: Drift-Cyclotron coordinates

Drift motion (large) ~ beam spot size and solenoid field

$$\vec{d} = \vec{r} - \vec{\rho} = \begin{pmatrix} x \\ y \end{pmatrix} - \frac{\beta_s}{2}\begin{pmatrix} y' \\ -x' \end{pmatrix} \qquad \beta_s = \frac{eB_z}{2\gamma\beta mc}$$

Cyclotron motion (small) ~ thermal emittance

$$\vec{k}_\perp = \gamma\beta\begin{pmatrix} x' \\ y' \end{pmatrix}$$

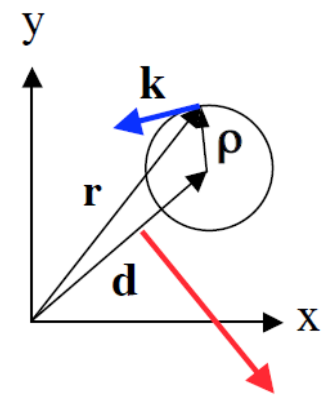

4D Transverse emittance:

$$(r, r', \theta, \theta'): \quad \varepsilon_{4D} = (\gamma\beta)^2\left[\langle r^2\rangle\langle r'^2 + (r\theta')^2\rangle - \langle rr'\rangle^2 - \langle r^2\theta'\rangle^2\right]$$

$$(d_x, d_y, k_x, k_y): \quad \varepsilon_{4D} = \frac{1}{4}\langle d^2\rangle\langle k_\perp^2\rangle = \varepsilon_{drift}\varepsilon_{cyclotron} \qquad \varepsilon_{drift} >> \varepsilon_{cyclotron}$$

Propagation in Rotational Symmetric Beamlines (preserves CAM)

$$M = \begin{pmatrix} A & B \\ -B & A \end{pmatrix} = R(\theta_M)\begin{pmatrix} D & 0 \\ 0 & D \end{pmatrix}$$

Rotational symmetry of beamline

$$\Sigma = \begin{pmatrix} \langle XX^T \rangle & \langle XY^T \rangle \\ \langle YX^T \rangle & \langle YY^T \rangle \end{pmatrix} \qquad R(\theta)\cdot\Sigma\cdot R^{-1}(\theta) = \Sigma$$

Rotational symmetry of beam matrix

Beam matrix representation under propagation

$$\Sigma_0 = \begin{pmatrix} T_0 & L_0 J \\ -L_0 J & T_0 \end{pmatrix} \xrightarrow{M} \Sigma = R(\theta_M)\begin{pmatrix} D T_0 D^T & L_0 J \\ -L_0 J & D T_0 D^T \end{pmatrix} R(-\theta_M)$$

All radial dynamics contained here.

Invariants under M: DetΣ , -1/2 Tr ($\Sigma J \Sigma J$)

(D.D. Holm, *et. al.*, J. Math. Phys. **31** (7), 1990.
Also: Cayley-Hamilton Thm.)

Normal mode emittances: $\varepsilon_- = \varepsilon_x - L_0$, $\varepsilon_+ = \varepsilon_x + L_0$

Normal Mode Emittances

Normal modes carry different angular momenta

$$\varepsilon_{4D} = \frac{1}{4}\langle d^2\rangle\langle k_\perp^2\rangle = \varepsilon_{drift}\varepsilon_{cyclotron} = \varepsilon_+\varepsilon_-$$

Transport of normal mode emittances follows oscillations in radial emittance

Laminar flow

$$2\varepsilon_\pm = \pm\langle rp_t\rangle + \sqrt{\langle r^2\rangle\langle p_t^2 + p_n^2\rangle - \langle rp_n\rangle^2} = \pm\langle M\rangle + \sqrt{(2\varepsilon_r)^2 + \langle M^2\rangle}$$

Conserved after initial transient

Oscillates at plasma frequency

Conserved after initial transient

Radial Dynamics Governed by Quasi-Laminar Flow

The radial rms envelope equation

$$\sigma_r'' + \sigma_r'\left(\frac{\gamma'}{\gamma\beta^2}\right) + k_{eff}^2\sigma_r - \frac{\kappa_s}{\sigma_r\gamma^3\beta^3} - \frac{\varepsilon_{nr}^2}{\sigma_r^3\gamma^2\beta^2} - \left(\frac{\langle p_\theta\rangle}{mc\gamma\beta}\right)^2\frac{1}{\sigma_r^3} = 0$$

admits a non-trivial equilibrium solution:

$$\sigma_{eq}^2 = \left(\frac{\kappa_s}{2k_{eff}^2}\right)\left[1+\left(1+\mu^2\right)^{1/2}\right]$$

$$\mu = 2\frac{k_{eff}\varepsilon_{eff}}{\gamma\beta\kappa_s}\begin{cases}\Rightarrow 0 & \text{Space-charge dominated beam}\\ \Rightarrow \infty & \text{'Emittance' dominated beam}\end{cases}$$

where

$$k_{eff}^2 = \frac{\gamma''}{2\gamma\beta^2} + \left(\frac{qB_z}{\gamma\beta mc}\right)^2$$

Effective focusing

(rf + magnetic)

$$\varepsilon_{eff}^2 = \varepsilon_{nr}^2 + \langle p_\theta\rangle^2 \Big/ (mc)^2$$

Effective emittance

(emittance + CAM)

$$\kappa_s = \frac{I_b/I_0}{(\gamma\beta)^3}$$

Perveance

(space charge)

Magnetized beam envelope and emittances

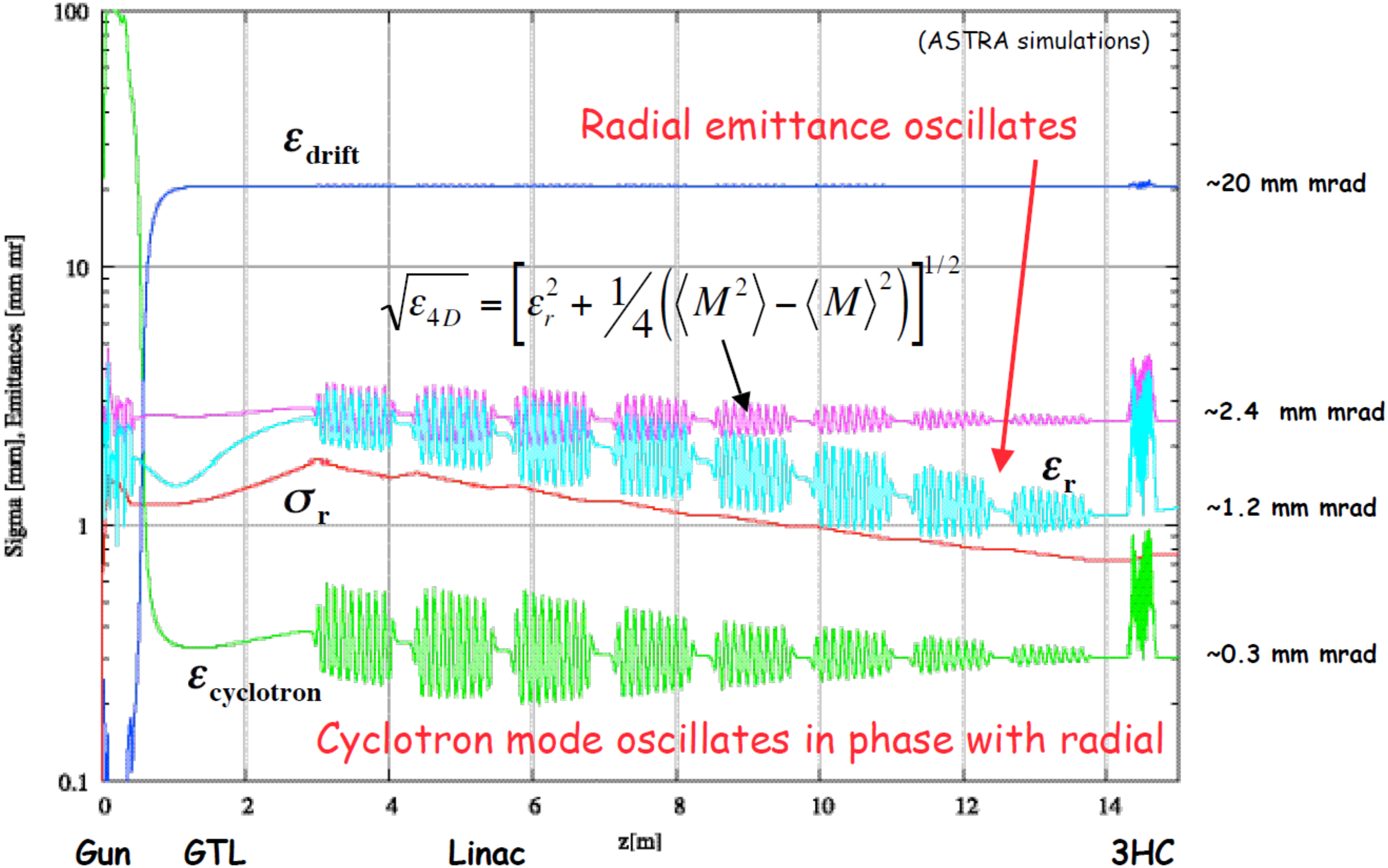

Flat Beam Injectors

To produce flat beams with the current approach requires us to operate the photoinjector in a new configuration.

A strong magnetic solenoid field is applied to the cathode.

The evolution of the launched beam is dominated now by both angular momentum and space charge forces. The beam dynamics within the rf gun is significantly different than previous designs.

For a beam with initial canonical angular momentum, the normal modes in the RF gun, GTL, and Linac are the drift and cyclotron motions.

The radial emittance of the round beam is important to track for space charge induced growth and emittance compensation.

In the Adapter beamline, rotational symmetry is broken and the normal modes are horizontal and vertical.

In a system with linear forces, the total transverse 4D emittance is conserved and the flat beam Adapter lattice converts the former set of normal modes into the latter.

Drift -> Horizontal, Cyclotron -> Vertical

Obtaining Vertical Emittances << Initial Thermal Emittance

The horizontal to vertical emittance ratio is related to the initial angular momentum and the initial thermal emittance:

$$\frac{\varepsilon_x}{\varepsilon_y} = 1 + 2\frac{(eB_z)^2}{(2\gamma\beta mc)^2}\frac{\langle x_0^2 + y_0^2\rangle}{\langle x_0'^2 + y_0'^2\rangle} = 1 + \frac{1}{2}\left(\frac{1}{2}\frac{eB_z}{mc}\right)^2\frac{\langle r_0^2\rangle^2}{\varepsilon_{thermal}^2} = 1 + \frac{1}{2}\frac{\langle p_\theta / mc\rangle^2}{\varepsilon_{thermal}^2}$$

To make this ratio large requires:

$$\left\langle \frac{p_\theta}{mc} \right\rangle \approx \frac{1}{2}\frac{eB_z}{mc}\langle r_0^2\rangle >> \sqrt{2}\ \ \varepsilon_{thermal} \propto \sqrt{\langle r_0^2\rangle}\sqrt{\langle r_0'^2\rangle}$$

The inequality can be satisfied easily by increasing the spot size at the cathode or the magnetic field at the cathode, or both.

Flat beam adapter – general scheme

- Generic quad lattice transfer matrix: $$T = \begin{pmatrix} A & 0 \\ 0 & B \end{pmatrix}$$

- Generic skew quad transfer matrix: $$N = R^{-1}TR = \frac{1}{2}\begin{pmatrix} A+B & A-B \\ A-B & A+B \end{pmatrix}$$

- Flat (horizontal) beam transform: $$\begin{pmatrix} X_2 \\ Y_2 \end{pmatrix} = N\begin{pmatrix} X_1 \\ Y_1 \end{pmatrix} = \frac{1}{2}\begin{pmatrix} (A+B)X_1 + (A-B)Y_1 \\ (A-B)X_1 + (A+B)Y_1 \end{pmatrix}$$

- Adapter requires: $$(A-B)X_1 + (A+B)Y_1 = 0$$

90° relative phase advance between A and B

Skew quadrupole triplet is simplest lattice that accomplishes this.

PHYSICAL REVIEW E **66**, 016503 (2002)

Circular modes, beam adapters, and their applications in beam optics

Alexey Burov* and Sergei Nagaitsev
Fermi National Accelerator Laboratory, Batavia, Illinois 60510

Yaroslav Derbenev†
Jefferson National Accelerator Facility, Newport News, Virginia 23606

(Received 13 June 2001; revised manuscript received 18 March 2002; published 30 July 2002)

Bema Matrix and Correlations

- 4D Beam Sigma matrix

$$\Sigma = \begin{pmatrix} \langle XX^T \rangle & \langle XY^T \rangle \\ \langle YX^T \rangle & \langle YY^T \rangle \end{pmatrix} = \begin{pmatrix} \Sigma_X & \Sigma_X C \\ C^T \Sigma_X & \Sigma_Y \end{pmatrix}$$

- Beam is initially correlated by solenoid field

$$C_0 = \begin{pmatrix} 0 & -\frac{2}{eB_0} \\ \frac{eB_0}{2} & 0 \end{pmatrix}$$

- Correlation matrix propagates through beam line

$$C_0 \Rightarrow C = \begin{pmatrix} a & b \\ c & d \end{pmatrix} = \begin{pmatrix} a & b \\ \frac{1+a^2}{b} & -a \end{pmatrix}$$

Symmetry: Unimodular & Rotational

Analytical results for simple 3-skew-quadruple adapter

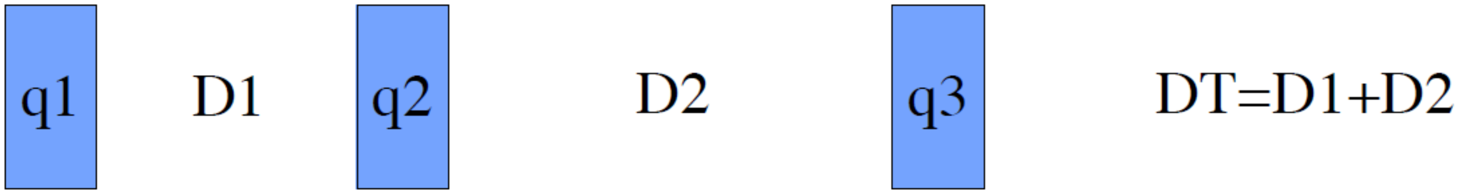

- Correlation matrix at channel entrance $$C_1 = \begin{pmatrix} a & b \\ c & d \end{pmatrix}$$

- Quad strengths determined by solving $$(A-B)+(A+B)C_1 = 0$$

$$q_1 = \pm\sqrt{\frac{-D_1 a + b - D_1 D_T c + D_T d}{D_1 D_T b}},$$

$$q_2 = -\frac{b + D_T d}{D_1 D_2 (1 + q_1 b)},$$

$$q_3 = -\frac{q_1 + q_2 + D_1 q_1 q_2 a - c}{1 + (D_T q_1 + D_2 q_2)a + D_1 D_2 q_2 (q_1 + c)}.$$

(+) for Horizontal beam
(-) for Vertical beam

Envelope and emittances in Adapter

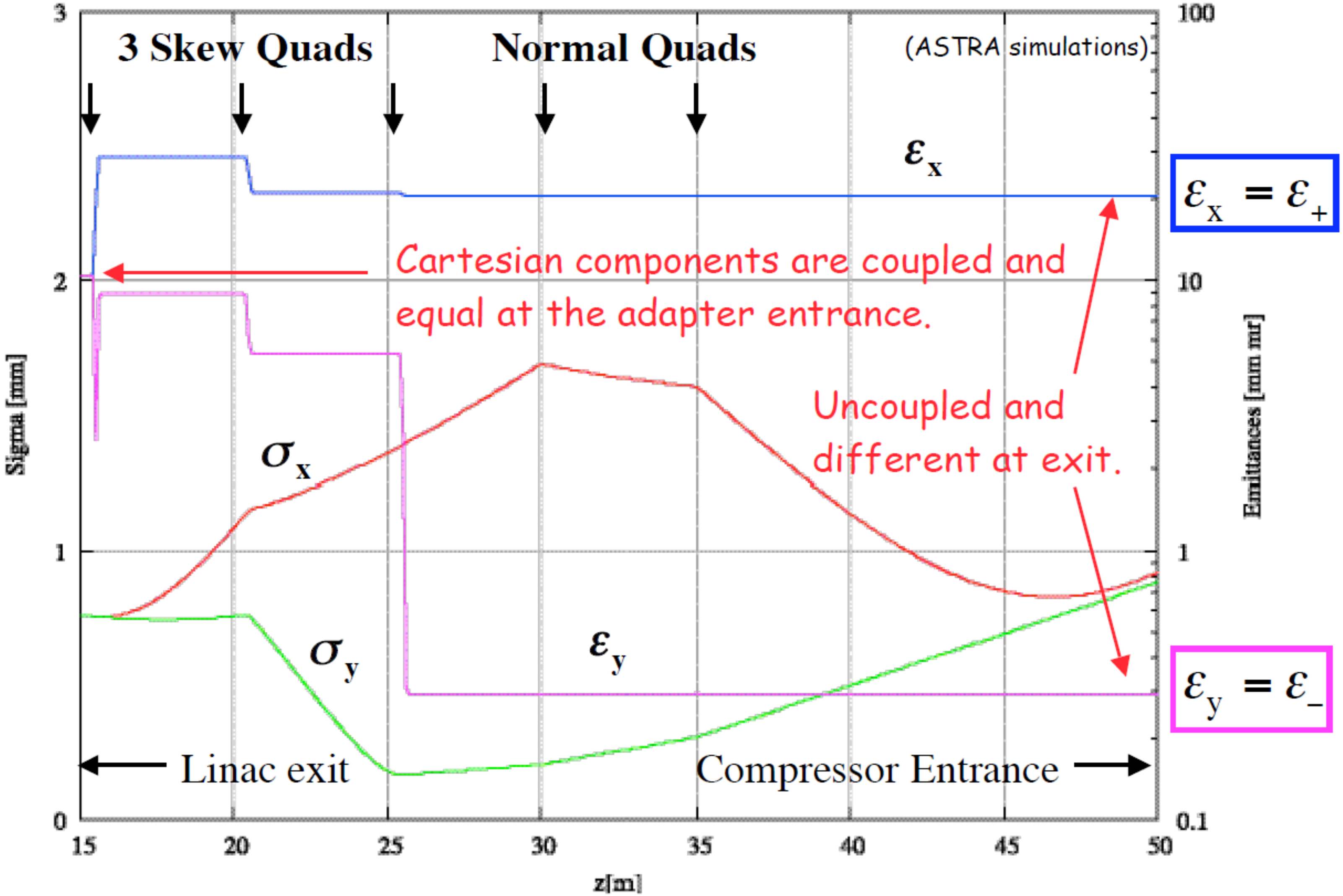

Evolution of Correlation Matrix in Adapter